Rapid warming and ostracods mass extinction at the Lower Toarcian (Jurassic) of central Spain

J.J. Gómez [a,*], C. Arias [b]

[a] Dpto. de Estratigrafía, Facultad de Ciencias Geológicas (UCM) and Instituto de Geología Económica (CSIC-UCM), 28040 Madrid, Spain
[b] Dpto. de Paleontología, Facultad de Ciencias Geológicas (UCM) and Instituto de Geología Económica (CSIC-UCM), 28040 Madrid, Spain

Keywords:
Palaeoclimate
Stable isotopes
Ostracods
Mass extinction
Early Toarcian

ABSTRACT

Here we present the results of the study of two Lower Toarcian carbonate sections located in the Iberian Range of central Spain. Analyses of stable isotope on belemnite calcite allowed calculation of seawater palaeotemperature variations, which were compared with the stratigraphical distribution of ostracods. These organisms are particularly sensitive to ratios of temperature and salinity variations and hence are good indicators of climate changes. From a cooling interval, with seawater temperatures of 13.2 °C recorded at the Pliensbachian—Toarcian transition, seawater temperature began to rise in the lowermost Toarcian Tenuicostatum Zone, reaching average temperatures between 14.6 °C and 16.3 °C during the time of deposition of this Zone. Coinciding with this seawater warming, up to 85% of the ostracods species progressively disappeared during a period of approximately 300 kyr, marking the extinction interval. The extinction boundary, located around the Tenuicostatum—Serpentinum zonal boundary, coincides with a marked increase in temperature in the Serpentinum Zone, on which average seawater temperatures of 22 °C have been calculated. Warming continued through part of the Middle Toarcian Bifrons Zone, reaching average temperatures of 24.7 °C. Readjustment of the ostracod population allowed recovery of these faunas in the upper Serpentinum Zone, although the extinction of a major ostracod group, the healdioids, was also recorded. The correlation between mass extinction and warming infers a causal relationship. Comparison of the results with the records of stable isotopes in belemnites and in bulk carbonates, as well as TOC and facies analysis suggests that the anoxia linked to the Early Toarcian oceanic anoxic event was not the main responsible for the ostracod mass extinction.

1. Introduction

Many biotic crises of Earth's history were suggested as past analogues for future biotic changes in course of Global Change (Fraiser, 2009). Therefore, the fossil record offers excellent opportunities to analyze the strong links between past rapid climate changes and their effects on floral and faunal extinctions (e.g. Kennett and Stott, 1991; Courtillot and Gaudemer, 1996; Culver and Rawson, 2000; Benton and Twitchett, 2003; Mayhew et al., 2008; Gómez et al., 2008, 2009) and in some cases the records of the lag time needed for a later recovery.

A warming interval that occurred in the Lower Toarcian (183—181.2 Ma; Ogg, 2004; Ogg et al., 2008) of the Lower Jurassic, has been recorded in different areas of Western Europe such as the UK (Jenkyns et al., 1991; Sælen et al., 1996; McArthur et al., 2000; Jenkyns, 2003), Germany (Röhl et al., 2001; Schmid-Röhl et al., 2002), France (Dera et al., 2009), Bulgaria (Metodiev and Koleva-Rekalova, 2008), Spain (Rosales et al., 2003, 2004; Gómez et al., 2008) and Portugal (Suan et al., 2008). Synchronously with this warming interval, a significant mass extinction event occurred. Generally this event is defined as a geologically brief interval (i.e. ~1 Ma) of elevated extinction rates that affected diverse taxa throughout the world (Hallam and Wignall, 1997). It has been reported in several areas, affecting many groups of fossils (e.g. Hallam, 1961, 1986, 1987, 1996; Arias et al., 1992; Little and Benton, 1995; Aberhan and Fürsich, 1997; Harries and Little, 1999; Pálfy and Smith, 2000; Cecca and Macchioni, 2004; Gómez et al., 2008). Synchronism between mass extinction and climate change infers that warming was the main cause of marine faunal extinction.

Deposition of organic-rich black shale facies during the Early Toarcian in some areas has been interpreted as the result of a synchronous and widely distributed major Early Toarcian Oceanic Anoxic Event (ETOAE) (Jenkyns, 1985, 1988, 1999, 2003; Jenkyns and Clayton, 1986, 1997; Jenkyns et al., 1994, 2001, 2002; Jiménez et al., 1996; Mailliot et al., 2006) and assumed by many authors to be one of the main causes of the mass extinction (e.g. Jenkyns, 1988; Nikitenko and Shurygin, 1992; Bassoullet and Baudin, 1994; Harries and Little, 1999; Pálfy and Smith, 2000; Jenkyns et al., 2002; Vörös, 2002; Aberham and Baumiller, 2003; Tremolada et al., 2005; Wignall et al.,

---

* Corresponding author. Tel.: +34 913944783; fax: +34 913944808.
E-mail addresses: jgomez@geo.ucm.es (J.J. Gómez), cariasf@geo.ucm.es (C. Arias).

2005; Mailliot et al., 2009). However, reappraisal through high-resolution stratigraphy indicates that the ETOAE is diachronous at the ammonite zone/subzone scale and only occasionally coincident with the mass extinction boundary (Wignall et al., 2005; Gómez et al., 2008; McArthur et al., 2008).

We here present the results of a study of two particularly well exposed Lower Toarcian carbonate sections, as a contribution aimed to elucidate the causes of this mass extinction event. The sections were previously well dated with ammonites at the subzone scale, and are located in the Iberian Range of central Spain (Fig. 1 a, b): the La Almunia section and the Sierra Palomera section. Analyses of stable isotope of diagenetically screened belemnite calcite and bulk carbonates, as well as total organic carbon (TOC) analysis, together with the stratigraphical distribution of ostracods, have been performed in both sections. Ostracods have been selected, as they are organisms particularly sensitive to temperature and salinity variations and hence good indicators of climate changes (Arias, 2007). The results obtained have been compared to test the relationship between seawater palaeotemperature variations and ostracods faunal turnovers, but the possible influence of the ETOAE in the recorded mass extinction is also analyzed.

2. Regional setting

The Iberian Range is a NW—SE oriented folded and thrusted belt (Fig. 1b) that resulted from the tectonic inversion during the Cenozoic. During the Early and Middle Jurassic, a system of carbonate platforms, the Iberian platform system, developed in this area of central Spain under a post-rift extensional tectonic regime. Active tectonics favoured the presence of syn-sedimentary faulted blocks and the extrusion of volcanic deposits along some of the active faults, mainly during the Toarcian but also during the early part of the Middle Jurassic (Gómez and Goy, 2004, 2005; Gómez and Fernández-López, 2004, 2006). The Upper Pliensbachian is mainly represented by the bioclastic limestones of the Barahona Fm (Fig. 2), but progressive deepening of the platform in the Lower Toarcian conditioned the deposition of the open-marine hemipalagic alternating limestones and marls of the Turmiel Fm. This progressive flooding of the platform culminated in the mid-Toarcian peak transgression of Cycle LJ-3 that was recorded in the Bifrons Zone (Fig. 2).

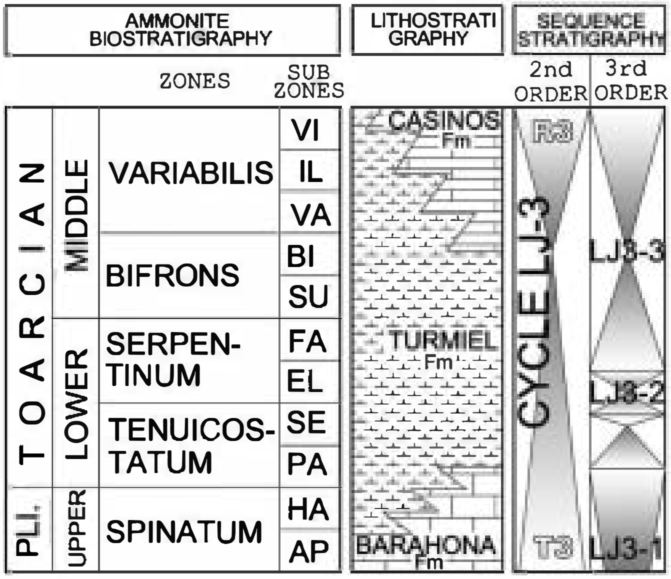

Fig. 2. Stratigraphic framework of the uppermost Pliensbachian—Lower and Middle Toarcian of the Iberian Range. Most of the Lower Toarcian deposits are represented by an alternation of hemipelagic marls and lime mudstones of the Turmiel Fm. The Upper Pliensbachian and the Lower—Middle Toarcian deposits reflect the transgressive interval of the 2nd order Cycle LJ-3. However, at a more detailed scale, smaller 3rd order cycles including shallowing intervals can be recognized. Subzones abbreviations: AP — Apyrenum. HA — Hawskerense. PA — Paltum. SE — Semicelatum. EL — Elegantulum. FA — Falciferum. SU — Sublevisoni. BI — Bifrons. VA — Variabilis. IL — Illustris. VI — Vitiosa.

3. Materials and methods

The sections have been studied bed by bed and ostracods from 15 samples collected at the La Almunia section and 14 samples from the Sierra Palomera section were prepared and studied following conventional methods. Samples used in this study are almost exclusively from mudstones and marls. The sample processing consisted of drying, weighing out 100 g of sample material and dispersing in a solution of hydrogen peroxide, sodium hydroxide and water. The disintegrated samples were washed through sieves with mesh diameter of >60, 125, 250, 500 and 1000 μm. All ostracods from

Fig. 1. Location of the studied sections. (a) Map showing the location of the Iberian Range. (b) Outcrops of the Jurassic deposits in Central Spain and location of the La Almunia and the Sierra Palomera sections.

the >125, 250, 500 and 1000 μm fractions were picked and mounted onto cardboard microscope slides. The fraction >60 μm was tested, revealing little influence on diversity and composition.

Sixty-seven belemnites were prepared for analyses of stable isotope. In addition, a total of 62 bulk carbonate samples were collected and analyzed for C and O isotope ratios, and 23 samples were analyzed for total organic carbon (TOC). For the assessment of possible burial diagenetic alteration of the collected belemnites, polished samples and thick sections of each belemnite rostra were prepared. The thick sections were studied under the petrographic and the cathodoluminescence microscope. Only the non-luminescent portions of the belemnite guards were sampled using a microscope-mounted dental drill. Sampling of the luminescent parts such as the apical line and the outer phragmocone wall, fractures, stylolites and borings have been avoided. Additionally, 30 belemnite calcite samples were analyzed using X-ray diffraction techniques to make sure that no other minerals except for calcite were present in the samples. A part of the belemnites collected at La Almunia were analyzed for stable isotopes at the Salamanca University (Spain) and the remaining belemnite and bulk rock samples at the University of Michigan (USA). Carbonate samples weighing a minimum of 10 micrograms were placed in stainless steel boats. Samples were roasted at 200 °C in vacuum for 1 h to remove volatile contaminants and water. Samples were then placed in individual borosilicate reaction vessels and reacted at 77° ± 1 °C with 3 or 4 drops of anhydrous phosphoric acid for 8 minutes in a Finnigan MAT Kiel IV preparation device coupled directly to the inlet of a Finnigan MAT 253 triple collector isotope ratio mass spectrometer. O^{17} corrected data are corrected for acid fractionation and source mixing by calibration to a best-fit regression line defined by two NBS standards, NBS 18 and NBS 19. Precision and accuracy of data were monitored through daily analysis of powdered carbonate standards. At least six standards were analyzed daily, bracketing the sample suite at the beginning, middle, and end of the day's run. In all samples, isotope ratios are reported in per mil relative to the standard Peedee belemnite (PDB). Several samples were analyzed in both laboratories. Reproducibility between both laboratories was better than 0.4‰ PDB for $\delta^{13}C$ and better than 0.6‰ PDB for $\delta^{18}O$. Internal analytical precision in belemnite carbonates was ±0.04‰ for both $\delta^{13}C$ and $\delta^{18}O$, and internal analytical precision in bulk carbonates was ± 0.04‰ for $\delta^{13}C$ and ±0.09‰ for $\delta^{18}O$. TOC analyses have been performed in the Centro de Espectrometría Atómica of the Universidad Complutense of Madrid using a Shimadzn TOC-V analyzer for solid samples (SSM-5000 A). One sample of standard NIST 1944 was analyzed every four samples of rock to control the total carbon values and bicarbonate of soda for the inorganic carbon. Analytical error was better than ±0.7%.

The Toarcian seawater palaeotemperatures recorded in the belemnite rostra have been calculated using the equation of Anderson and Arthur (1983):

$$T(^\circ C) = 16.0 - 4.14\ (\delta_c - \delta_w) + 0.13\ (\delta_c - \delta_w)^2$$

where $\delta_c = \delta^{18}O$ PDB is the composition of the sample, and $\delta_w = \delta^{18}O$ SMOW is the composition of ambient seawater. Normal values of $S = 34.3‰$ for the marine salinity (Wright, 1987) and δ_w values of −1‰ for a non-glacial ocean water were used (Sackleton and Kennet, 1975).

4. Results

4.1. La Almunia section

The Lower Toarcian deposits have been studied along a hillside near the town of La Almunia (Fig. 3) (Lat. 41° 28′ 54″N, Long. 1° 24′ 51″W). The lowermost part of the Toarcian is represented by bioclastic wackestones to packstones of the Barahona Fm, but most of the Lower Toarcian is represented by the hemipelagic alternating lime mudstone and marls of the Turmiel Fm (Fig. 4). Ammonite biostratigraphy at the subzone scale has been based on the results of Goy and Martínez (1990), Goy et al. (1996) and Gómez et al. (2008).

4.1.1. Stable isotope records

Plotting of the $\delta^{13}C_{bel}$ and $\delta^{18}O_{bel}$ as well as the $\delta^{13}C_{bulk}$ and $\delta^{18}O_{bulk}$ values in this section against the stratigraphical levels shows significant variations along the studied interval (Fig. 4). The overall trend of the $\delta^{13}C_{bel}$ values describe a positive excursion, with a peak value of 3.1‰ reached in the Falciferum Subzone (Serpentinum Zone). Two minor negative $\delta^{13}C_{bel}$ peaks are recorded. The lower shift is located in the uppermost Tenuicostatum Zone, and the upper negative excursion is recorded in the Middle Toarcian Bifrons Subzone, where negative values as low as −0.34‰ are reached. The $\delta^{13}C_{bulk}$ curve shows scattered values, probably in part altered by burial diagenesis, but average values in the Semicelatum Subzone are 1.3‰ and average values at the Elegantulum Subzone are 0.9‰, marking a minor negative shift of about 0.3‰.

The $\delta^{18}O_{bel}$ values significantly vary in the studied interval. In the lowermost Toarcian (Tenuicostatum Zone), values are more negative than in the uppermost Pliensbachian, from −0.3‰ at the end-Pliensbachian to −1.7‰ as an average around the Tenuicostatum–Serpentinum zonal boundary. That marks the onset of a significant excursion towards more negative values that starts at the Tenuicostatum–Serpentinum zonal boundary and that reaches a prominent peak value in the Elegantulum Subzone. Additional shifts have been recorded higher in the section, in the Middle

Fig. 3. Partial view of the Lower Toarcian alternation of limestone and marl of the Turmiel Fm at La Almunia. Shed is about 2 m high.

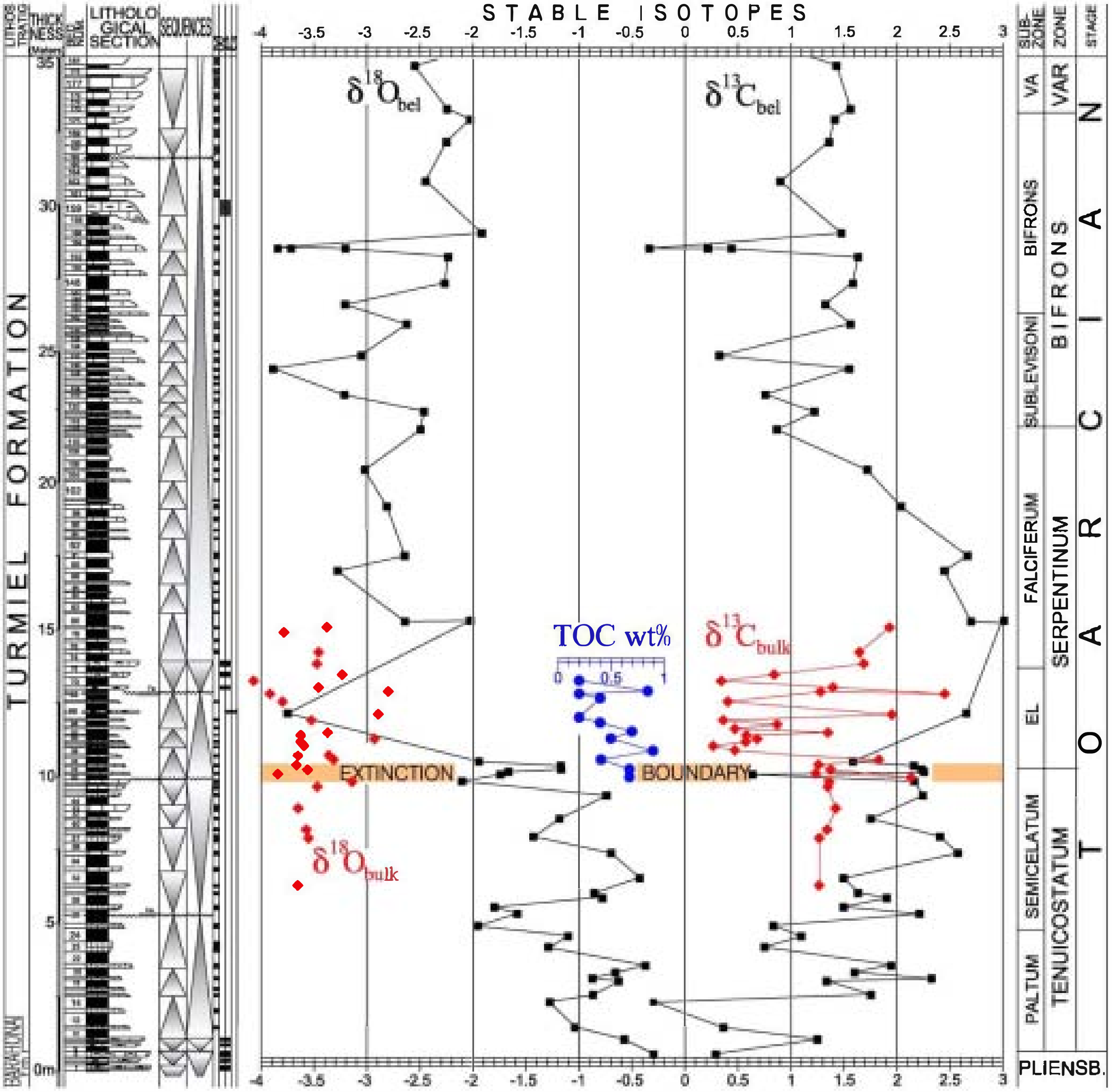

Fig. 4. Stratigraphic column of the uppermost Pliensbachian and the Lower/Middle Toarcian deposits in the La Almunia section, showing sequence stratigraphy and the curves of the stable isotopes based on belemnite calcite ($\delta^{18}O_{bel}$ and $\delta^{13}C_{bel}$) and in bulk carbonates ($\delta^{18}O_{bulk}$ and $\delta^{13}C_{bulk}$) as well as the total organic carbon (TOC) concentration. Zones abbreviations: VAR – Variabilis. Subzones abbreviations: EL – Elegantulum. VA – Variabilis.

Toarcian Bifrons Subzone, coinciding with the $\delta^{13}C_{bel}$ negative excursion. The $\delta^{18}O_{bulk}$ values obtained from carbonates are quite uniform, showing an average value of −0.36‰, which reflects the signal acquired during burial diagenesis.

4.1.2. TOC values

Marls of the uppermost Semicelatum Subzone and of the Elegantulum Subzone have been analyzed for TOC content. All samples of the interval supposedly corresponding to the ETOAE show values below 1 wt.% and more than a half of the samples have less than 0.5 wt.% TOC (Fig. 4). Based on these results, and taking into account that for many authors black shales should contain more than 5 wt.% TOC (Bates and Jackson, 1987; Kearey, 2001; McArthur et al., 2008) these deposits can hardly be classified as organic-rich black shale facies, which for many authors are the diagnostic representatives of the Early Toarcian Oceanic Anoxic Event (Jenkyns, 1985, 1988, 1999, 2003; Jenkyns and Clayton, 1986, 1997; Jenkyns et al., 1994, 2001, 2002; Jiménez et al., 1996; Mailliot et al., 2006). Marls and carbonates

Fig. 5. Stratigraphical distribution of ostracods (modified after Arias, 1995, 1996), and other benthic organisms in the uppermost Pliensbachian–Lower Toarcian in the La Almunia section. The progressive loss of species during the Tenuicostatum Biochron represents the extinction interval, (following the nomenclature of Kauffman and Erwin, 1995). The mass extinction boundary is located around the Tenuicostatum–Serpentinum zonal boundary. Above the extinction boundary, the population interval is marked by the appearance of new taxa. Brachiopod data modified after García Joral and Goy (1996). Bivalves distribution modified after Bernad (1996). EL–Elegantulum Subzone.

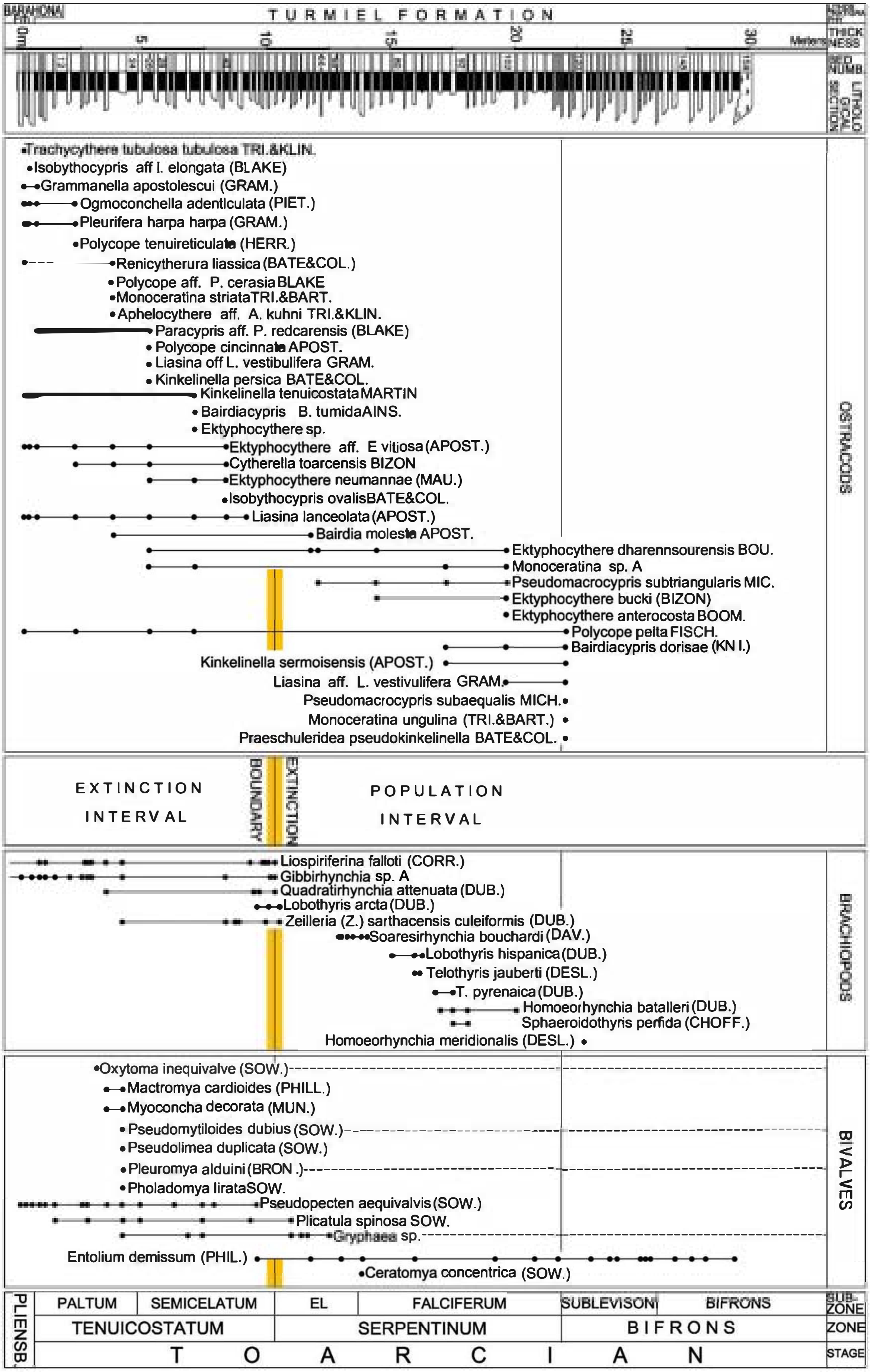
BARAHONA FM.
TURMIEL FORMATION
THICKNESS
0m
5
10
15
20
25
30
Meters
BED NUMB.
LITHOLOGICAL SECTION
Trachycythere tubulosa tubulosa TRI.&KLIN.
Isobythocypris aff I. elongata (BLAKE)
Grammanella apostolescui (GRAM.)
Ogmoconchella adenticulata (PIET.)
Pleurifera harpa harpa (GRAM.)
Polycope tenuireticulata (HERR.)
Renicytherura liassica (BATE&COL.)
Polycope aff. P. cerasia BLAKE
Monoceratina striata TRI.&BART.
Aphelocythere aff. A. kuhni TRI.&KLIN.
Paracypris aff. P. redcarensis (BLAKE)
Polycope cincinnata APOST.
Liasina off L. vestibulifera GRAM.
Kinkelinella persica BATE&COL.
Kinkelinella tenuicostata MARTIN
Bairdiacypris B. tumida AINS.
Ektyphocythere sp.
Ektyphocythere aff. E vitiosa (APOST.)
Cytherella toarcensis BIZON
Ektyphocythere neumannae (MAU.)
Isobythocypris ovalis BATE&COL.
Liasina lanceolata (APOST.)
Bairdia molesta APOST.
Ektyphocythere dharennsourensis BOU.
Monoceratina sp. A
Pseudomacrocypris subtriangularis MIC.
Ektyphocythere bucki (BIZON)
Ektyphocythere anterocosta BOOM.
Polycope pelta FISCH.
Bairdiacypris dorisae (KN I.)
Kinkelinella sermoisensis (APOST.)
Liasina aff. L. vestivulifera GRAM.
Pseudomacrocypris subaequalis MICH.
Monoceratina ungulina (TRI.&BART.)
Praeschuleridea pseudokinkelinella BATE&COL.
OSTRACODS
EXTINCTION INTERVAL
BOUNDARY
EXTINCTION
POPULATION INTERVAL
Liospiriferina falloti (CORR.)
Gibbirhynchia sp. A
Quadratirhynchia attenuata (DUB.)
Lobothyris arcta (DUB.)
Zeilleria (Z.) sarthacensis culeiformis (DUB.)
Soaresirhynchia bouchardi (DAV.)
Lobothyris hispanica (DUB.)
Telothyris jauberti (DESL.)
T. pyrenaica (DUB.)
Homoeorhynchia batalleri (DUB.)
Sphaeroidothyris perfida (CHOFF.)
Homoeorhynchia meridionalis (DESL.)
BRACHIOPODS
Oxytoma inequivalve (SOW.)
Mactromya cardioides (PHILL.)
Myoconcha decorata (MUN.)
Pseudomytiloides dubius (SOW.)
Pseudolimea duplicata (SOW.)
Pleuromya alduini (BRON.)
Pholadomya lirata SOW.
Pseudopecten aequivalvis (SOW.)
Plicatula spinosa SOW.
Gryphaea sp.
Entolium demissum (PHIL.)
Ceratomya concentrica (SOW.)
BIVALVES
PLIENSB.
PALTUM
SEMICELATUM
EL
FALCIFERUM
SUBLEVISONI
BIFRONS
SUBZONE
TENUICOSTATUM
SERPENTINUM
BIFRONS
ZONE
TOARCIAN
STAGE

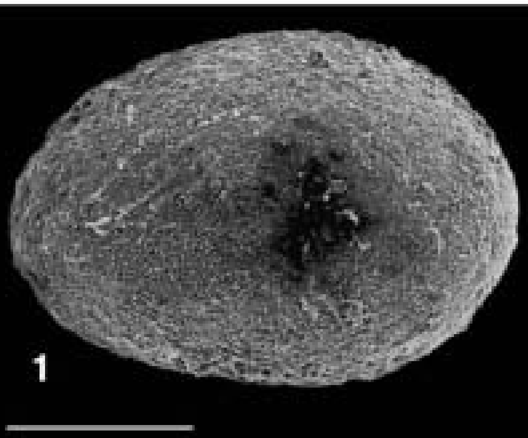
1

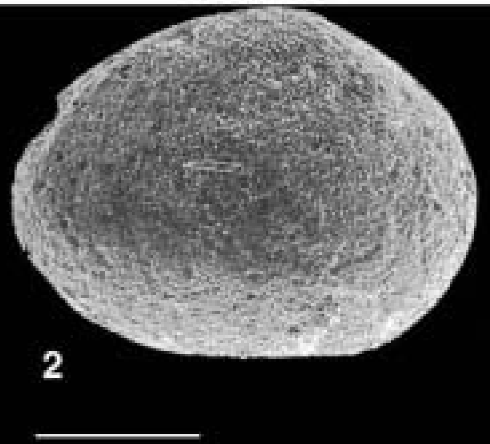
2

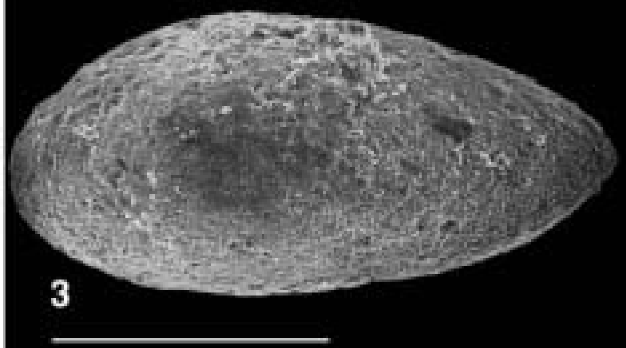
3

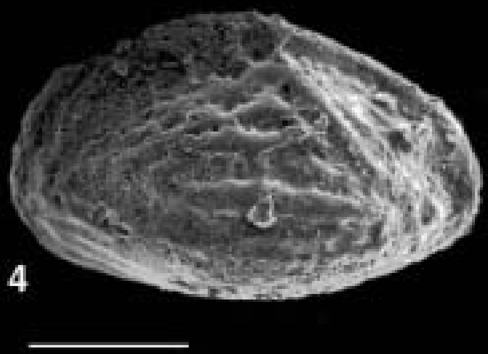
4

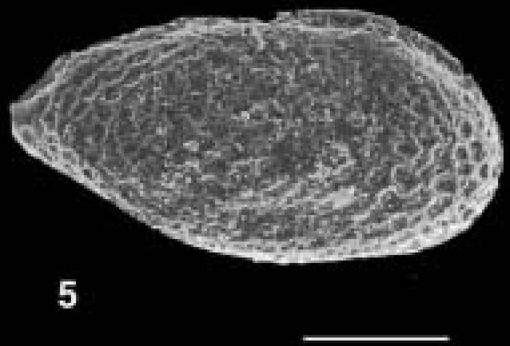
5

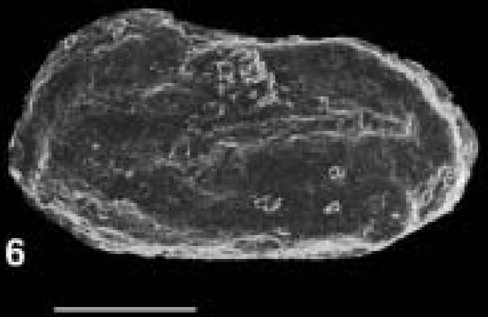
6

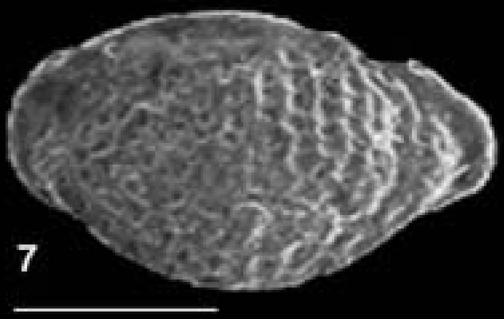
7

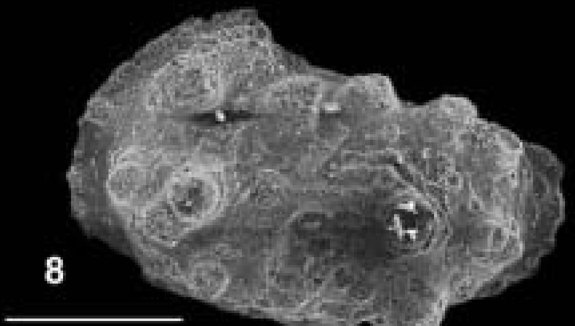
8

of the studied interval show bioturbated fabrics, except for a level of marls located in the Serpentinum Zone, above the extinction interval, that shows parallel lamination.

4.1.3. Ostracods record

Noteworthy changes in the distribution of taxa in the uppermost Pliensbachian–Lower Toarcian interval have been recorded in the La Almunia section (Arias, 1995, 1996). From a total of 35 ostracods taxa identified in this section, 26 taxa that had their First Appearance Datum (FAD) before the Tenuicostatum–Serpentinum zonal boundary, only 4 (15%) surpassed this boundary, while 22 taxa (85%) progressively disappear in the Lower Toarcian Tenuicostatum Zone. After an interval probably equivalent to the lower part of the Elegantulum Zone, where no new appearances were recorded, 6 taxa originated in the Serpentinum Zone.

The well marked interval in which 85% of the ostracods taxa disappeared (uppermost Pliensbachian and lowermost Toarcian Tenuicostatum Zone) corresponds to the "extinction interval" defined by Kauffman and Erwin (1995) (Fig. 5) and, as many authors have pointed out, the extinction boundary can be clearly marked around the Tenuicostatum–Serpentinum zonal boundary (e.g. Hallam, 1987; Arias et al., 1992; Little and Benton, 1995; Harries and Little, 1999; Cecca and Macchioni, 2004; Wignall et al., 2005, 2006; Gómez et al., 2008).

The pronounced ostracod faunal turnover is manifested by the replacement of the typical Pliensbachian ostracod assemblages dominated by healdioids, large cytheroids of the genera *Gramannella* and *Pleurifera*, and a few species of the genera *Cytherella, Bairdiacypris, Polycope, Monoceratina, Eucytherura* and *Pseudomacrocypris*. The ostracod assemblages that recovered from the lowest part of the Semicelatum Subzone show an important faunal turnover (Fig. 5), with the most typical Late Pliensbachian–Early Toarcian ostracod species (*Liasina lanceolata* (Plate 1, Fig. 1), *Cytherella toarcensis*, *Liasina vestibulifera*, *Gramannella apostolescui* (Plate 1, Fig. 5), *Ektyphocythere* aff. *E. vitiosa* (Plate 1, Fig. 4), *Kinkelinella tenuicostata* and *Pleurifera harpa harpa* (Plate 1, Fig. 6)) progressively disappearing and being replaced by a few cytheroids species (*Kinkelinella sermoisensis*, *Ektyphocythere anterocosta*, *Ektyphocythere bucki* and *Bairdiacypris dorisae*) as the main component of the assemblages. Therefore, the Serpentinum Zone seems to represent the end of the renewal period. This period is marked by the healdioid extinction (Lord, 1982; Boomer et al., 2008), a group that appeared in the Devonian, and persisted until the Lower Toarcian Serpentinum Zone, and the replacement of cypridoid and cytherellid by cytheroids, which became dominant, making up 90% of the total ostracod faunal assemblages.

Other groups such as the brachiopods and bivalves studied at La Almunia show a similar stratigraphical distribution pattern, marking the mass extinction interval. The mass extinction boundary is also well marked by the ostracods, the bivalves and the brachiopods. The population interval is indicated by the first appearance of new species of ostracods and brachiopods in the Elegantulum Subzone (Fig. 5).

4.2. Sierra Palomera section

The Sierra Palomera section has been studied along the Rambla del Salto creek (Fig. 6) (Long. 40° 37′ 20″ N; Lat. 2° 27′ 40″ W), located north of the Teruel town (Fig. 1 b). The lithostratigraphical units corresponding to the uppermost Pliensbachian and the Lower–Middle Toarcian are the same as the mentioned for La Almunia (Fig. 7). The ammonite biostratigraphy, performed at the subzone scale, is based on Comas-Rengifo et al. (1996) and Osete et al. (2007).

Fig. 6. General view of the Toarcian deposits, represented by the Turmiel Fm, in the Sierra Palomera section. For scale, total thickness of the Turmiel Fm is near 65 m.

4.2.1. Stable isotope records

Stable isotope data at Sierra Palomera have been obtained from belemnites and from bulk carbonates. However, belemnites are extremely scarce above the Tenuicostatum–Serpentinum zonal boundary (the extinction boundary) and only a fragmented low-resolution isotopic record from belemnite calcite can be observed above this level. Variations of $\delta^{13}C_{bel}$ and $\delta^{18}O_{bel}$ as well as of the $\delta^{13}C_{bulk}$ and $\delta^{18}O_{bulk}$ values recorded in this section and plotted against the stratigraphical levels are shown in Fig. 7.

The $\delta^{13}C_{bel}$ values clearly increase in the Tenuicostatum Zone and tend to slightly decrease in the scarce values recorded in the Serpentinum and Bifrons zones. This marks a prominent positive excursion that is also recorded in the $\delta^{13}C_{bulk}$ curve, showing peak values around the boundary between the Elegantulum and the Falciferum subzones. Within the positive excursion recorded in the $\delta^{13}C_{bulk}$ carbonates, a clear negative shift, located around the Tenuicostatum–Serpentinum zonal boundary, is evident from several samples.

The $\delta^{18}O_{bel}$ values progressively shift towards more negative values in the Tenuicostatum Zone and the scarce values above the Tenuicostatum–Serpentinum zonal boundary tend to be more negative than the values recorded below this boundary. Even the $\delta^{18}O_{bulk}$ values, reflecting the burial diagenesis effect, show a similar trend to the $\delta^{18}O_{bel}$ curve. Values tend to be more negative in the Tenuicostatum Zone, reaching the peak of the negative excursion close to the Tenuicostatum–Serpentinum zonal boundary.

4.2.2. TOC values

TOC wt.% content of the Lower Toarcian marl beds reflects the lack of organic carbon in this part of the section except for two samples that returned values of up to 1.5 wt.% TOC (Fig. 7). These values are much lower than the minimum values (5 wt.% TOC) to be considered

---

Plate 1. Uppermost Pliensbachian and Lower Toarcian ostracods from the La Almunia and the Sierra Palomera sections. 1. *Ogmoconchella adendiculata* (Pietrzenuk, 1961). Right valve. Hawskerense Subzone, Spinatum Zone. SP.168.45. Sierra Palomera section. 2. *Ogmoconchella* aff. *O. aspinata* (Drexler, 1958). Left valve. Hawskerense Subzone, Spinatum Zone. SP.168.88. Sierra Palomera section. 3. *Liasina lanceolata* (Apostolescu, 1959). Left valve. Paltum Subzone, Tenuicostatum Zone. ADG.22.7. La Almunia section. 4. *Ektyphocythere* aff. *Ektyphocythere vitiosa* (Apostolescu, 1959). Left valve. Paltum Subzone, Tenuicostatum Zone. ADG.22.11. La Almunia section. 5. *Gramannella apostolescui* (Gramann, 1962). Carapace. Right lateral view. Peltum Subzone, Tenuicostatum Zone. ADG.14.7. La Almunia section. 6. *Pleurifera harpa harpa* (Klingler and Neuweiler, 1959). Left valve, Peltum Subzone, Tenuicostatum Zone. ADG.14.5. La Almunia section. 7. *Kinkelinella sermoisensis* (Apostolescu, 1959). Left valve. Semicelatum Subzone, Tenuicostatum Zone. SP.196.8. Sierra Palomera section. 8. *Trachycythere tubulosa tubulosa* (Triebel and Klingler, 1959). Left valve Semicelatum Subzone, Tenuicostatum Zone. SP.196.8. Sierra Palomera section. Scale bars = 100 μm long.

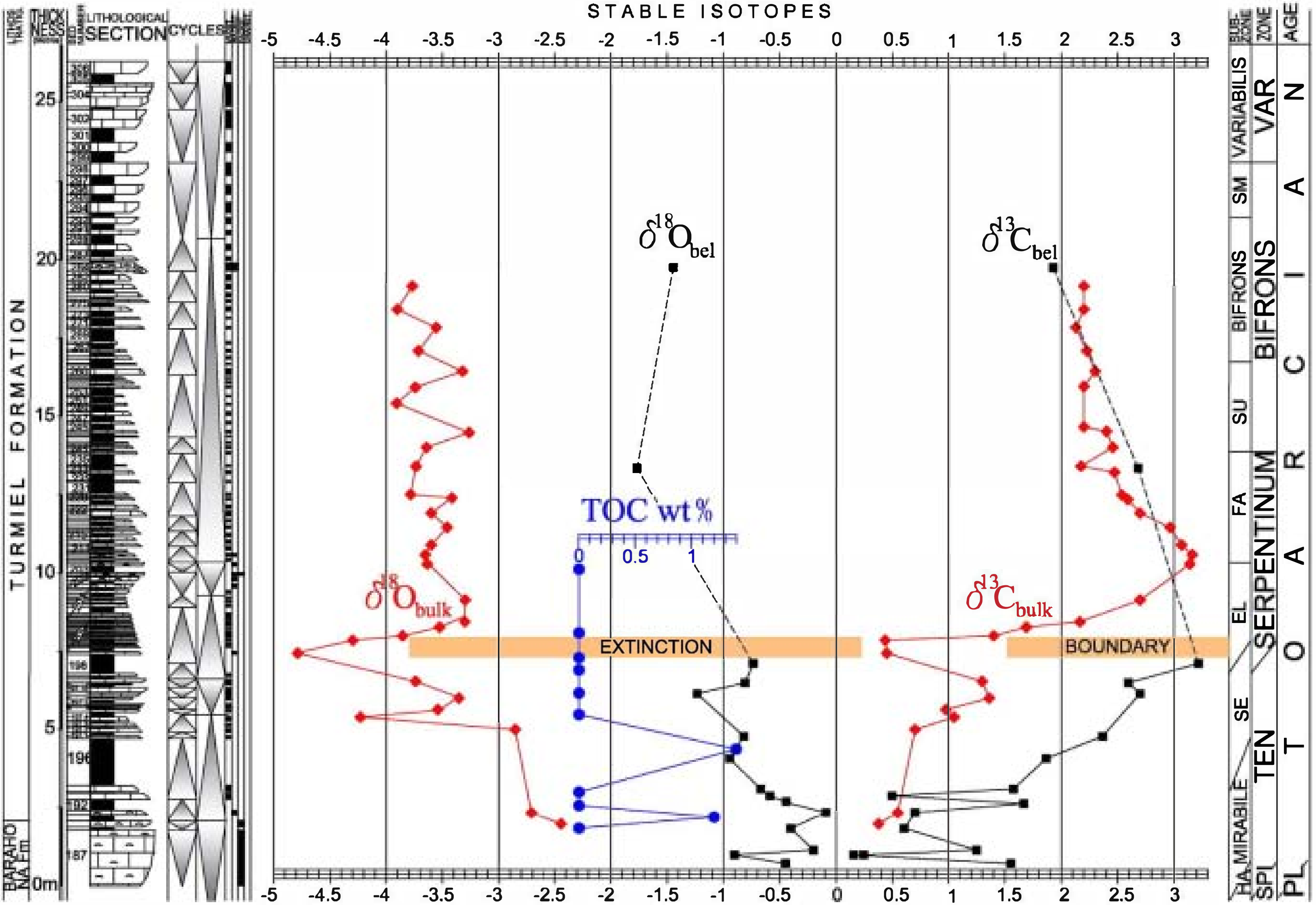

Fig. 7. Stratigraphic column of the uppermost Pliensbachian and the Lower/Middle Toarcian deposits of the Sierra Palomera section, showing sequence stratigraphy and the curves of the stable isotopes based on belemnite calcite ($\delta^{18}O_{bel}$ and $\delta^{13}C_{bel}$) and bulk carbonates ($\delta^{18}O_{bulk}$ and $\delta^{13}C_{bulk}$) as well as the total organic carbon (TOC) concentration. Zones abbreviations: SP – Spinatum. TEN – Tenuicostatum. VAR – Variabilis. Subzones abbreviations: HA – Hawskerense. SE – Semicelatum. EL – Elegantulum. FA – Falciferum. SU – Sublevisoni. SM – Semipolitum. VA – Variabilis.

as black shale facies (Bates and Jackson, 1987; Kearey, 2001; McArthur et al., 2008). The age of the thin intervals containing organic carbon do not coincide with the negative $\delta^{13}C$ excursion detected in bulk carbonates and is one biochron older than the slight enrichment in organic matter recorded at La Almunia section. The marls and the carbonates of the studied interval show bioturbated fabrics, and no laminated layers have been observed.

4.2.3. Ostracods record

Stratigraphical distribution of ostracods at Sierra Palomera (Fig. 8) shows a similar alternating numerical dominance of the cytheroids, and the cytherellids and a clear turnover pattern in the Tenuicostatum Zone as in the La Almunia section. From the 13 taxa that originated below the Tenuicostatum–Serpentinum zonal boundary, which as at La Almunia marks the extinction boundary, 10 taxa (77%) progressively disappeared (*Ogmoconchella adenticulata* (Plate 1, Fig. 1) and *Ogmoconchella* aff. *O. aspinata* (Plate 1, Fig. 2), marking the extinction interval, and three taxa survived the extinction event, marking the survival interval. This interval partly coincides with the period during which ostracods slowly recovered after the well marked extinction boundary. As a consequence, 5 new taxa had their FAD before the Bifrons Subzone (Fig. 8).

Among the 10 species that disappeared before the Tenuicostatum–Serpentinum transition, three of the most distinctive ostracod species previously described in the Tenuicostatum Zone (*Liasina lanceolata*, *Gramannella apostolescui* and *Ektyphocythere* aff *Ektyphocythere vitiosa)* are included, representing a significant renewal period, when Cytheroidea became dominant, constituting 100% of the total fauna in the Early Toarcian. As a result of the crisis, some new cytheroids species (*Ektyphocythere anterocosta, Praeschuleridea pseudokinkelinella, Trachycythere tubulosa tubulosa* (Plate 1, Fig. 8)) together with *Ektyphocythere bucki* and *Kinkelinella sermoisensis* (Plate 1, Fig. 7) became dominant in the Serpentinum Zone.

5. Discussion

To check that the $\delta^{13}C_{bel}$ and $\delta^{18}O_{bel}$ values can be interpreted as reflecting the original marine signal, with no evidence of significant diagenetic overprints, a cross-plot of the isotopic values has been performed (Fig. 9). The cluster type of distribution can be interpreted

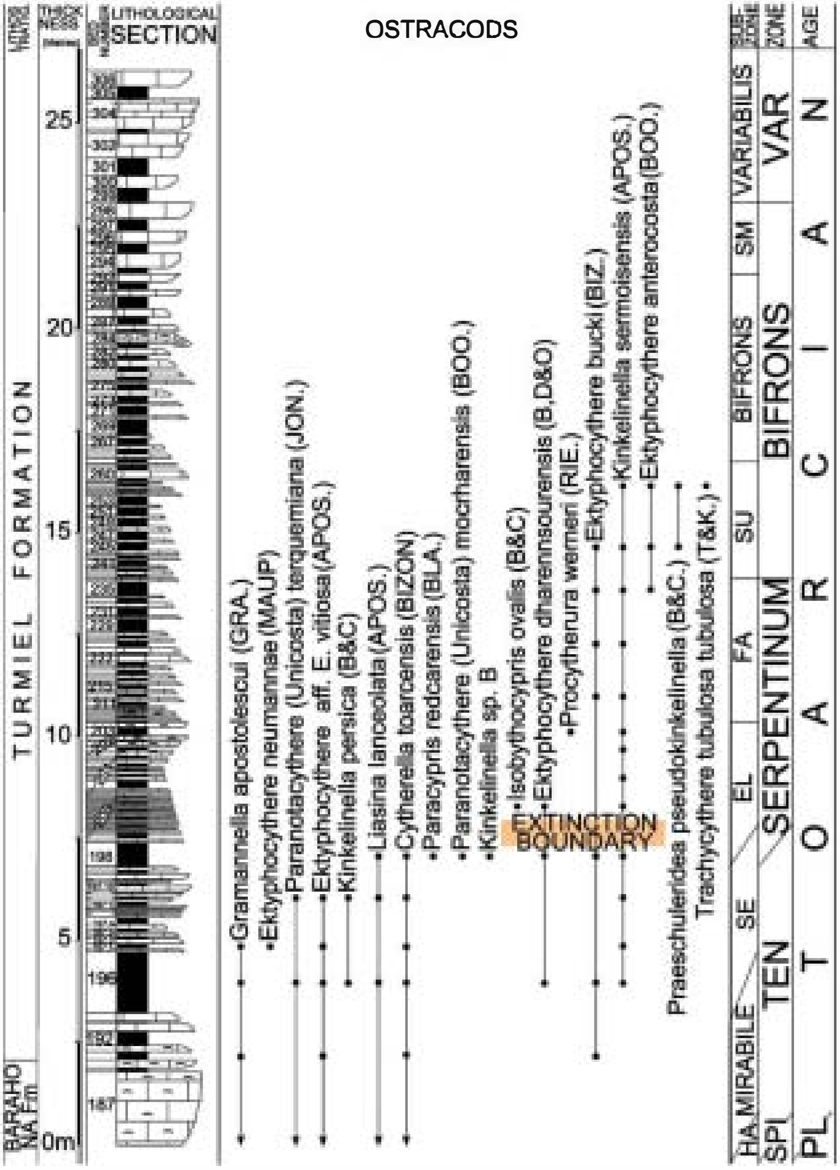

Fig. 8. Distribution of ostracods in the uppermost Pliensbachian and the Lower/Middle Toarcian deposits of the Sierra Palomera section. The mass extinction boundary is located around the Tenuicostatum – Serpentinum zonal boundary. Zones abbreviations: SP – Spinatum. TEN – Tenuicostatum. VAR – Variabilis. Subzones abbreviations: HA – Hawskerense. SE – Semicelatum. EL – Elegantulum. FA – Falciferum. SU – Sublevisoni. SM – Semipolitum. VA – Variabilis.

as indicative of no burial diagenetic overprint. However, the diagenesis observed in the bulk carbonates, luminescent in the cathodoluminescence microscope, is confirmed by the obtained isotopic values, which show a certain linear distribution around −3.5‰ PDB in the $\delta^{18}O_{bulk}$ values (Fig. 9).

5.1. Comparison of the $\delta^{13}C$ records

Comparison of the $\delta^{13}C_{bel}$ and $\delta^{13}C_{bulk}$ curves obtained in the La Almunia and in the Sierra Palomera sections, shows very similar features (Fig. 10). The $\delta^{13}C_{bel}$ values tend to increase in the uppermost Pliensbachian and in the lowermostToarcian. A notable increase starts in the upper Paltum/Mirabile Subzone, representing the onset of the remarkable positive excursion that develops up to the Falciferum Subzone in the La Almunia section. As in many other European sections, no evidence of a negative $\delta^{13}C_{bel}$ shift has been recorded in the belemnite calcite of this interval.

The $\delta^{13}C_{bulk}$ values also depict a significant positive excursion, which is more evident in the carbonates of the Sierra Palomera section. Peaks recorded in $\delta^{13}C_{bel}$ at the La Almunia section and in the $\delta^{13}C_{bulk}$ carbonates at Sierra Palomera show similar values, slightly above 3‰, and in both sections are recorded at the base of the Falciferum Subzone. Within the positive excursion, a 0.3 to 1‰ negative $\delta^{13}C_{bulk}$ shift has been recorded in both sections. Nevertheless, both negative excursions are diachronous. The negative excursion at Sierra Palomera starts near the Tenuicostatum–Serpentinum zonal boundary and develops in the lower half of the Elegantulum Subzone, while at La Almunia the onset of the negative shift occurs slightly later and develops in the Elegantulum Zone.

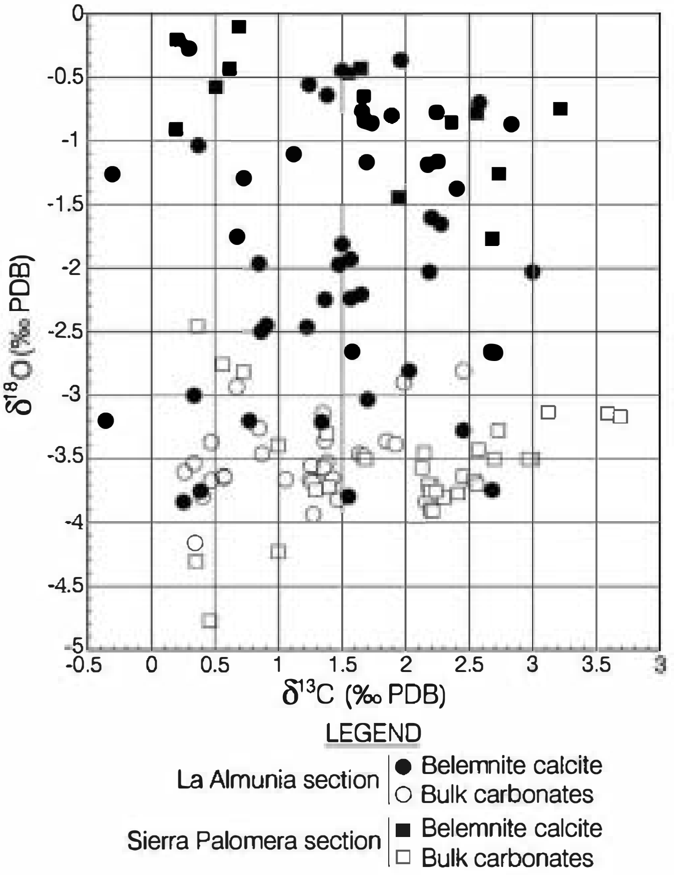

Fig. 9. Cross-plot of $\delta^{18}O$ and $\delta^{13}C$values, in ‰ PDB, obtained in belemnite calcite and in bulk carbonate samples from the uppermost Pliensbachian and the Lower Toarcian deposits in the La Almunia and in the Sierra Palomera sections. Most of the values obtained from belemnite calcite are well grouped into a cluster type of distribution, suggesting that they represent the original marine signal with lack of significant diagenetic overprints. On the contrary, data obtained from bulk carbonates show a preferential distribution around a value of −3.5‰ $\delta^{18}O$, confirming the diagenetic overprint observed under the cathodoluminescence microscope.

5.2. Timing of the Early Toarcian $\delta^{13}C$ excursions

The positive $\delta^{13}C$ excursion in the belemnite carbonate and, to a lesser extent, in the bulk rock samples recorded in the studied sections has also been reported from most European sections, whether in bulk rock, in belemnite calcite, in marine organic matter, and in wood (i.e. Jenkyns and Clayton, 1997, McArthur et al., 2000; Röhl et al., 2001; Jenkyns et al., 2002; Hesselbo et al., 2007a,b; Gómez et al., 2008). However, the timing of the $\delta^{13}C$ peak does not coincide in many of the considered sections of Europe at the ammonite zone/subzone scale (Gómez et al., 2008). As a consequence, the peak of this positive excursion should not be used as a chemostratigraphical correlative level, unless its synchronism is demonstrated with independent methods, such as magnetostratigraphy (Osete et al., 2007).

Many authors ascribe this shift to the response of water masses to excess and rapid burial of large amounts of organic carbon rich in ^{12}C that led to enrichment in ^{13}C of the inorganic carbon pool (Jenkyns, 1988; Jenkyns and Clayton, 1997; Schouten et al., 2000). Similar interpretation has been made for other positive $\delta^{13}C$ excursions, like for the Cenomanian–Turonian positive $\delta^{13}C$ excursion of northwest Europe, which is related to increased rates of organic carbon burial (Voigt et al., 2006). However, McArthur et al. (2000) explain the positive $\delta^{13}C$ excursion as the local response to the burial of organic matter and ebullition of isotopically heavy CO_2 to the overlying water column generated by methanogenesis of organic-rich deposits during shallow burial. Nevertheless, it should be considered that this positive excursion is also present in areas were no black shales were deposited. Examples are the $\delta^{13}C$ records obtained in the sections studied here, where no real black shale facies is present but the positive $\delta^{13}C$ excursion is recorded in belemnite calcite and in bulk carbonates. In addition, the timing of the positive $\delta^{13}C$ excursion does not coincide with the highest TOC values in many European sections (Parisi et al., 1996; Jiménez et al., 1996; Jenkyns and Clayton, 1997; Bucefalo Palliani et al., 1998; Duarte, 1998; Jenkyns et al., 2002; Schouten et al., 2000; Röhl etal, 2001; Rosales et al., 2001; Gómez et al., 2008; Mailliot et al., 2009), and in the sections presented here, as in many other European sections (e.g. Hesselbo et al., 2007a), the positive $\delta^{13}C$ excursion does not coincide with the presence of significant contents in organic carbon.

Referring to the up to 8‰ $\delta^{13}C$ negative excursion reported in many Lower Toarcian sections of NW Europe and Tethys, it has been recorded in bulk carbonates (Jenkyns and Clayton, 1997; Jenkyns et al., 2002; Schouten et al., 2000; Röhl et al., 2001; van de Schootbrugge et al., 2005; Tremolada et al., 2005; Hesselbo et al., 2007a,b; Gómez et al., 2008; Hermoso et al., 2009) and in organic matter (Jenkyns et al., 2001; Kemp et al., 2005; Hesselbo et al., 2007a,b; Röhl et al., 2001), but this negative $\delta^{13}C$ excursion seems to be diachronous with respect to the ammonites zonal scale (Gómez et al., 2008) and has not been clearly recorded in belemnite calcite (Sælen et al., 1996; McArthur et al., 2000; van de Schootbrugge et al., 2005; Wignall et al., 2005, 2006; McArthur, 2007; McArthur et al., 2008; Gómez et al., 2008; this work) suggesting to some authors that its global character is questionable (van de Schootbrugge et al., 2005).

5.3. Comparison of the $\delta^{18}O$ records and palaeotemperature calculation

Comparison of the $\delta^{18}O$ curves obtained in the two studied sections shows remarkable similarities (Fig. 11). From the slightly negative values recorded in the lowermost Toarcian, values are progressively more negative towards the top of the Tenuicostatum Zone. Coinciding with the Tenuicostatum–Serpentinum zonal

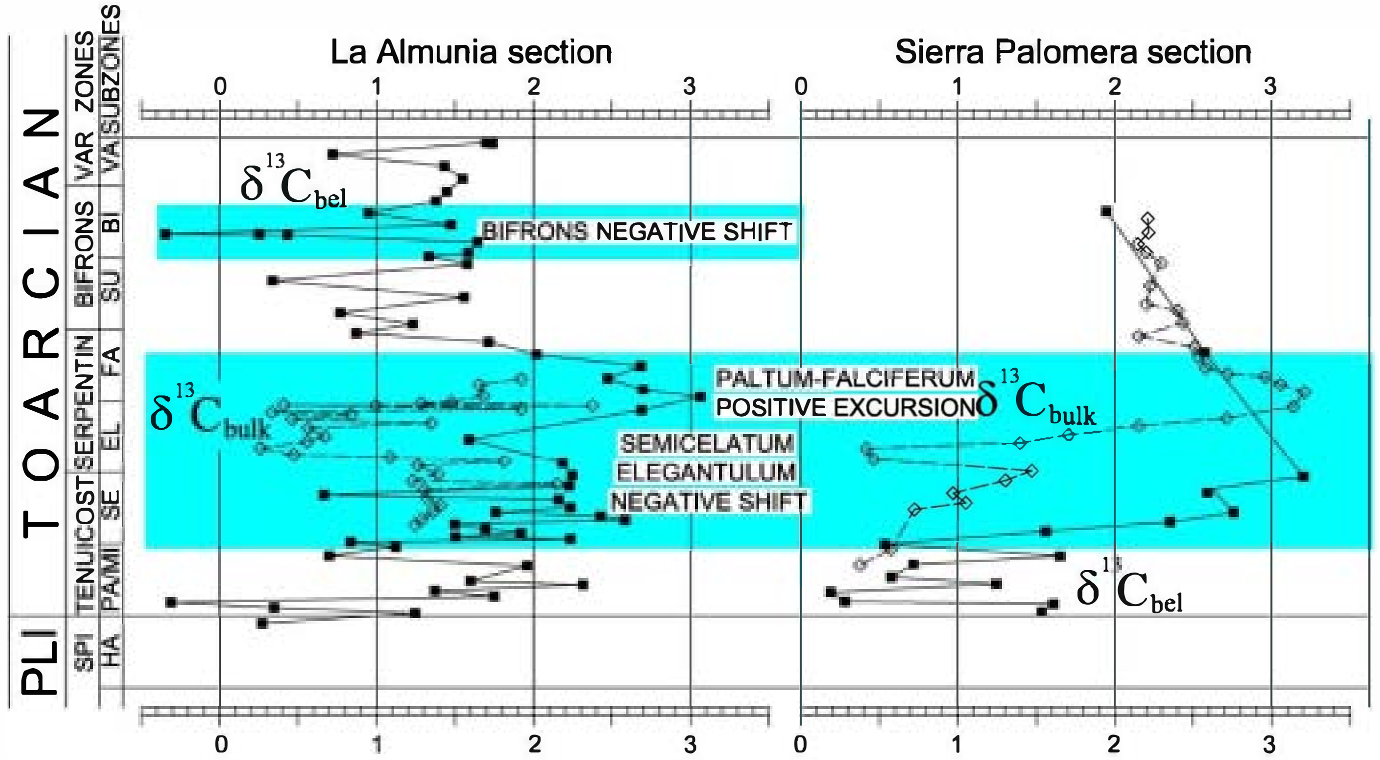

Fig. 10. Correlation chart of the uppermost Pliensbachian–Lower/Middle Toarcian $\delta^{13}C_{bel}$ and $\delta^{13}C_{bulk}$ curves obtained from the La Almunia and from the Sierra Palomera sections. Note the positive excursion starting in the lower Tenuicostatum Zone (Paltum/Mirabile Subzone) and extending up to the Falciferum Subzone of the Serpentinum Zone in the La Almunia section. From this positive shift, $\delta^{13}C_{bel}$ values tend to decrease, reaching negativevalues at La Almunia in the upper Bifrons Zone. The $\delta^{13}C_{bulk}$ curve of the Sierra Palomera section records a well defined negative excursion within the lower Elegantulum Subzone. The negative excursion is also recorded in the $\delta^{13}C_{bulk}$ curve at La Almunia, but at the Elegantulum and Falciferum subzones. This negative shift is not clearly marked in the belemnite calcite in both sections. Zones abbreviations: SPI – Spinatum. TENUICOST – Tenuicostatum. SERPENTIN – Serpentinum. VAR – Variabilis. Subzones abbreviations: HA – Hawskerense. PA – Paltum. MI – Mirabile. SE – Semicelatum. EL – Elegantulum. FA – Falciferum. SU – Sublevisoni. BI – Bifrons. VA – Variabilis. Note that for the lowermost Toarcian, the Paltum Subzone has been used at La Almunia due to the presence of the ammonites zone index *Protogrammoceras paltum* (BUCK.), while at Sierra Palomera this index has not been found and has been replaced by the index *Dactylioceras (Eodactylites) mirabile* FUC., which has a similar stratigraphic distribution.

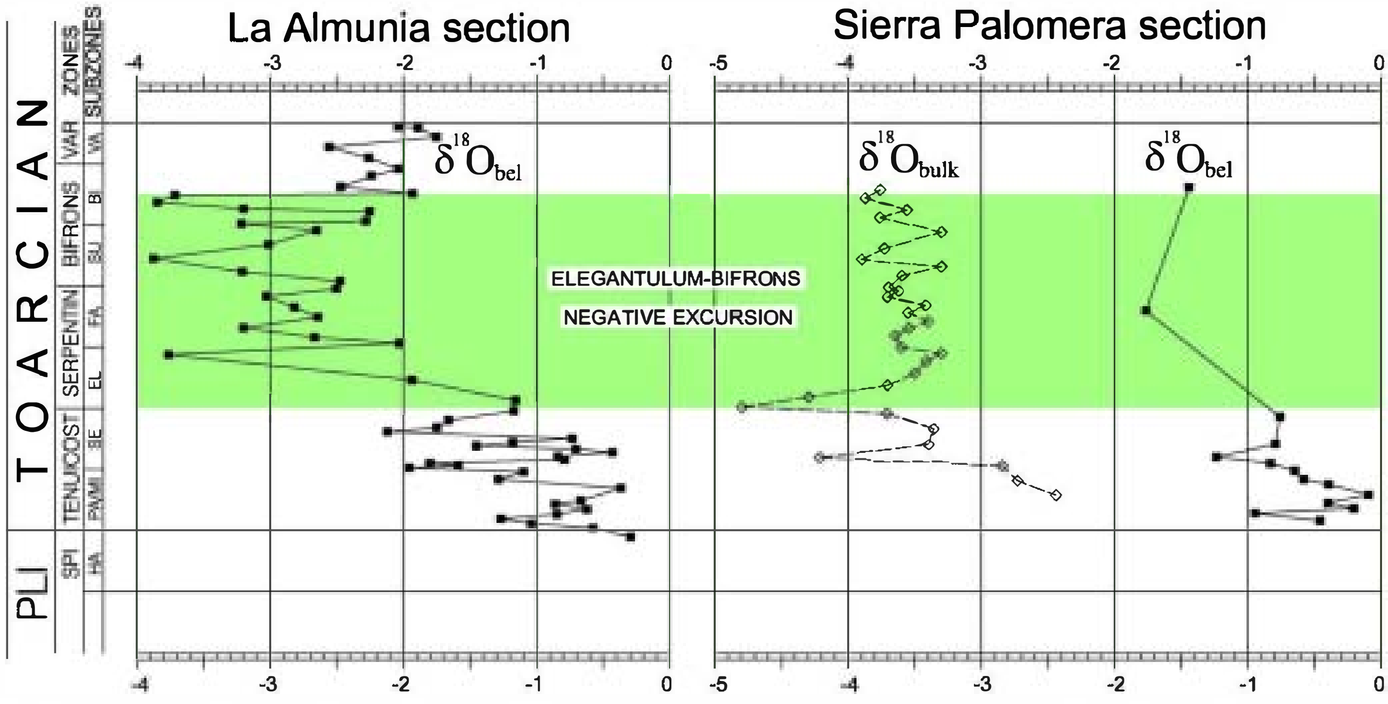

Fig. 11. Correlation chart of the uppermost Pliensbachian–Lower/Middle Toarcian $\delta^{18}O_{bel}$ curves obtained from the La Almunia and from the Sierra Palomera sections. A main negative excursion starts in the Tenuicostatum Zone, recorded in both sections, which rapidly develops in the Serpentinum Zone, up to the upper Bifrons Zone, mainly recorded in the LaAlmunia section. The $\delta^{18}O_{bulk}$ curve obtained at Sierra Palomera reflect values affected by burial diagenesis, but still seems to retain some of the original signal, showing a negative shift in the Tenuicostatum–Serpentinum zonal boundary. Zones abbreviations: SPI – Spinatum. TENUICOST – Tenuicostatum. SERPENTIN – Serpentinum. VAR – Variabilis. Subzones abbreviations: HA – Hawskerense. PA – Paltum. MI – Mirabile. SE – Semicelatum. EL – Elegantulum. FA – Falciferum. SU – Sublevisoni. BI – Bifrons. VA – Variabilis.

boundary (extinction boundary), a sudden and pronounced decrease in the $\delta^{18}O$ values marks a noteworthy negative excursion that develops up to the Bifrons Subzone. The negative excursion is well marked in the La Almunia section, but only one belemnite was studied from this interval in the Sierra Palomera section. Bulk carbonates at Sierra Palomera still retain some of the original signal of the negative excursion, although the $\delta^{18}O_{bulk}$ values clearly reflect the influence of the diagenetic overprint.

The Early Toarcian curve of seawater palaeotemperature variations in the two studied sections (Fig. 12a) was obtained by plotting the palaeotemperature values, calculated using as a proxy the $\delta^{18}O_{bel}$ obtained values, against the ammonites zones and subzones.

For palaeotemperature calculation, it has been assumed that the $\delta^{18}O$ values, and consequently the resultant curve, essentially reflects changes in environmental parameters (Sælen et al., 1996; McArthur et al., 2007), based on the assumption that the sampled non-luminescent biogenic calcite of the studied belemnite rostra precipitated in equilibrium with the seawater; that the biogenic calcite retains the primary isotopic composition of the seawater, and that the sampling bias, vital effects, skeletal growth and belemnite migration are not the main factors responsible for the obtained variations. The isotopic study of five different species of recent cuttlefish (*Sepia* sp.), the closest organisms to belemnite in current oceans, from seven different regions, evidenced that $\delta^{18}O$ values reflect the temperature of their habitat perfectly and that high salinity changes show no marked effect on the oxygen isotope signal of the cuttlebone (Rexfort and Mutterlose, 2009). These data support the reliability of the use of belemnite calcite as a proxi for palaeotempearature calculation, and its independence from salinity.

At the uppermost Pliensbachian Spinatum Zone, the palaeotemperatures obtained from the La Almunia section show relatively low values (13.2 °C), which are similar to those obtained by Rosales et al. (2004) in the Basque–Cantabrian Basin in Northern Spain, by Bailey et al. (2003) in Germany, and by Gómez et al. (2008) in central and northern Spain, indicating a relatively cool interval for the uppermost Pliensbachian–lowermost Toarcian.

The lowermost Toarcian Tenuicostatum Zone recorded marked oscillations of seawater temperature, but the overall temperatures tend to a progressive warming. The average palaeotemperatures, calculated from $\delta^{18}O_{bel}$ values, measured during the Tenuicostatum Biochron was 16.3 °C at La Almunia section and slightly lower (14.6 °C) at the Sierra Palomera section. However, at the top of the Tenuicostatum Zone, average temperatures of 18 °C with peak values up to 20.8 °C were reached, marking a first warming stage.

A remarkably rapid warming started around the Tenuicostatum–Serpentinum zonal boundary. Average temperature rose to 22 °C during the Serpentinum biochron and up to 24.7 °C as an average during most of the Bifrons Biochron. That represents a ΔT in the order of 5.7 °C during the Serpentinum Biochron and about 8.4 °C during the Bifrons Biochron, with respect to the temperatures recorded in the latest Pliensbachian–earliest Toarcian cool interval. During this warming episode, peak values of up to 29 °C were occasionally reached at La Almunia.

For a calculated palaeolatitude of Madrid of about 35–36° N during the Toarcian (Osete et al., 2000, in press) (Fig. 13 a, b), average palaeotemperatures reached during this warming interval were in the order of 5–8 °C higher than in the present-day oceans at a similar latitude (NOAA) but lower than the palaeotemperatures calculated for the Early Jurassic from climate modelling (Chandler et al., 1992).

5.4. Links between warming and ostracods extinction event

Detailed research of modern regional distribution of ostracods species from marine environments indicate that their distribution is strongly influenced by the water mass physico-chemical (e.g. temperature, salinity, nutrients, dissolved oxygen, etc) and substrate features (Benson et al., 1983; Whatley, 1988; Dingle and Lord, 1990; Cronin et al., 1994, 1995, 2002; Ayress et al., 2004). The close

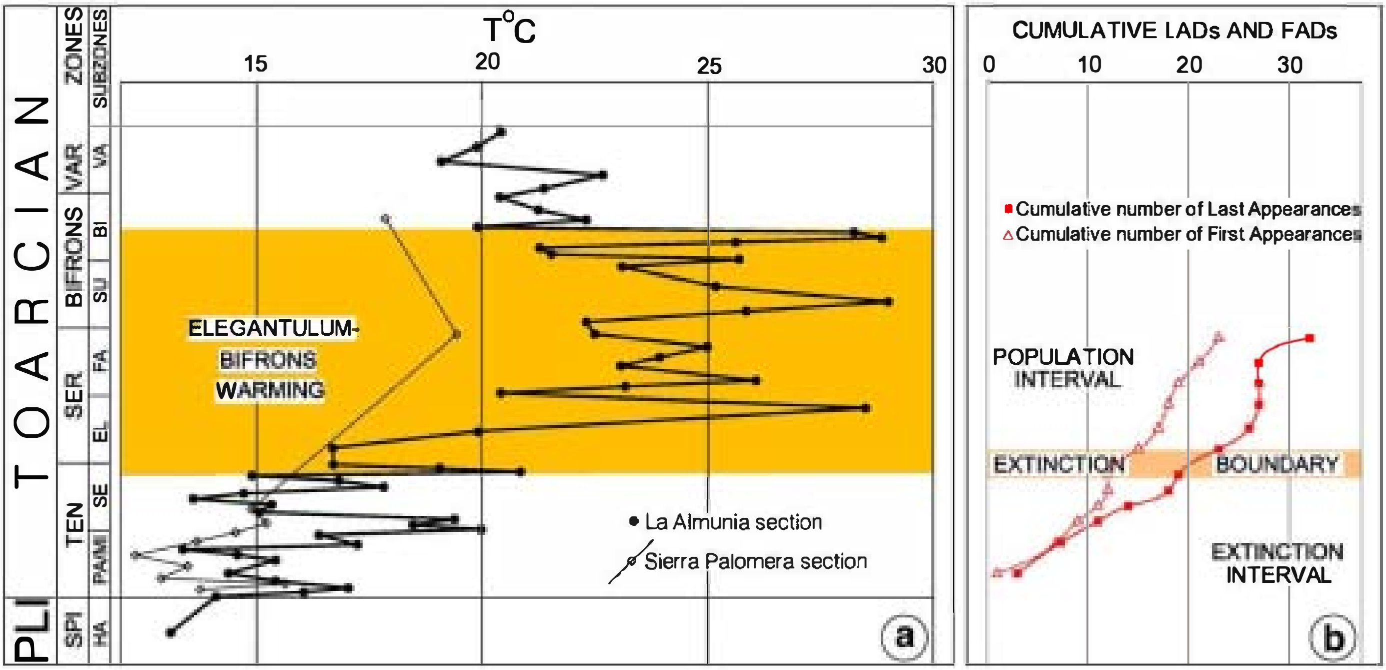

Fig. 12. (a) Curves of the latest Pliensbachian–Early/Middle Toarcian seawater palaeotemperatures obtained from $\delta^{18}O_{bel}$ values from the La Almunia and from the Sierra Palomera sections. (b) cross-plot of the cumulative number of Last Appearances Datum (LADs) and First Appearances Datum (FADs) of ostracods at the uppermost Pliensbachian and the Lower Toarcian. As temperature increases at the Tenuicostatum Zone, the number of LADs rapidly increases. Strong similarity between the seawater temperature and the extinction patterns supports that warming could be the cause of the mass extinction. The sudden increase of temperature at the Tenuicostatum–Serpentinum zonal boundary coincides with the extinction boundary. Ostarcods slowly recover during the Serpentinum Biochron, marking the population interval. Zones abbreviations: SPI – Spinatum. TEN – Tenuicostatum. SER – Serpentinum. VAR – Variabilis. Subzones abbreviations: HA – Hawskerense. PA – Paltum. MI – Mirabile. SE – Semicelatum. EL – Elegantulum. FA – Falciferum. SU – Sublevisoni. BI – Bifrons. VA – Variabilis.

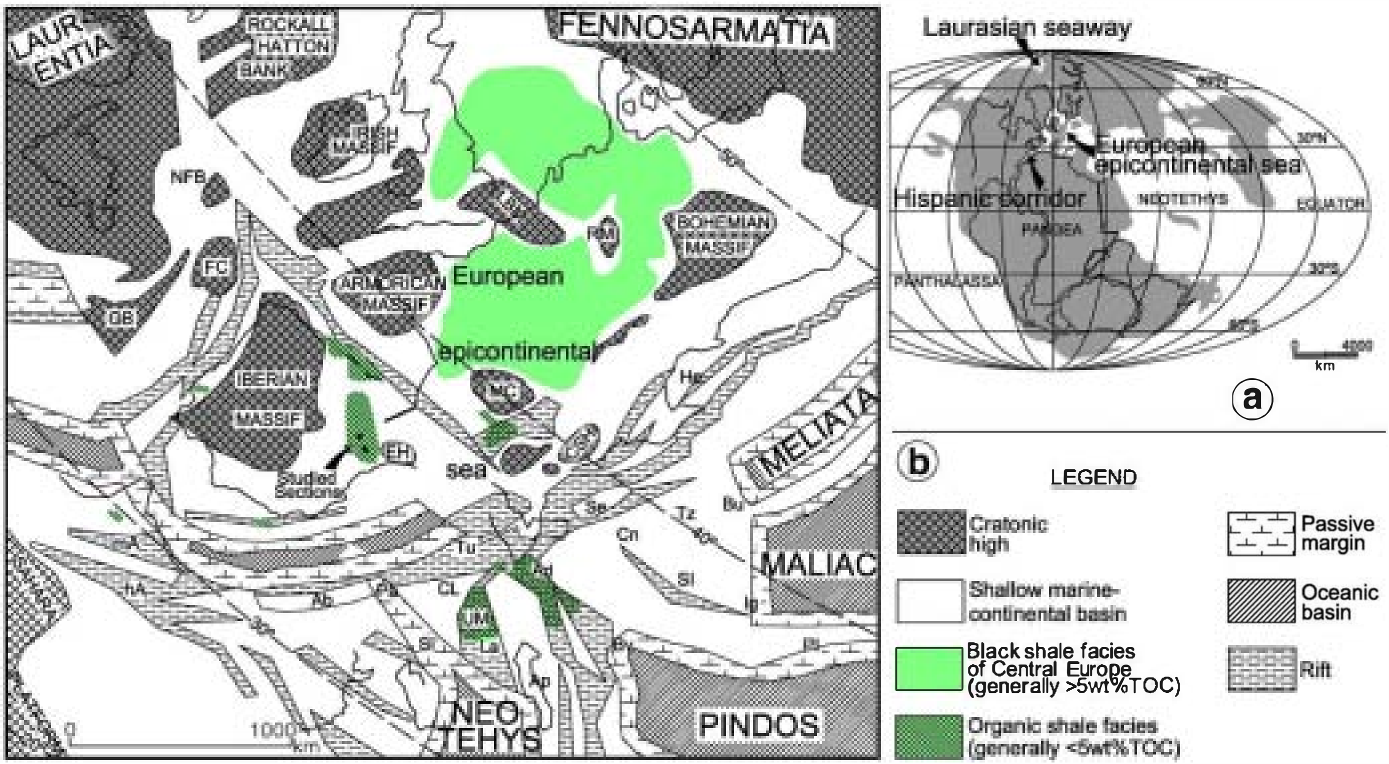

Fig. 13. Palaeogeography of the Toarcian. (a) Global palaeogeographical map of the Toarcian (modified after Golonka, 2006) showing the position of the Laurasian seaway, the European epicontinental sea (EES) and the Hispanic corridor. (b) Paleogeographical map of Western Tethys and the Proto-Atlantic Ocean (modified after Ziegler, 1990; Vera, 2001; Stampfli and Borel, 2004; Osete et al., in press) showing the position of the studied sections. The distribution of black shale, commonly laminated, facies of NW Europe is based on data from Jenkyns (1988), Bassoullet et al. (1991), Bucefalo Palliani et al. (1998), Vera (2001), van de Schootbrugge et al. (2005a, b), McArthur et al. (2008), Gómez et al. (2008). Real black shale laminated facies containing 5wt.% or more TOC are only common in Central Europe. The position and extension of the shales with some organic content in the Alpine–Mediterranean region is highly uncertain due to their sporadic occurrence, TOC values are generally below 3 wt.% and deposits are commonly bioturbated, indicating oxygenated bottom waters. However, Early Toarcian mass extinction has been recorded outside the areas covered by the black shale laminated facies, and no clear link between the presence of these black shales, representatives of the ETOAE or the RAE (Regional Anoxic Event (McArthur, 2007; McArthur et al., 2008) and mass extinction can be established. Abbreviations: Ab – Alboran. Ad – Adria s. str. Ap – Apulia s. str. Bu – Bucovinian. Bv-Budva. CL – Campania Lucania. Cn – Carnic-julian. EH-Ebro High. FC-Flemish Cap GB – Grand Bank. hA – High Atlas. He – Helvetic rim basin. Ig – Igal trough. La – Lagonegro. LBM –London-Braband Massif. mA – Middle Atlas. MC – Massif Central High. NFB – East Newfoundland Basin. Pa – Panormides. PI – Pelagonian. Se – Sesia (western Austroalpine). Si – Sicanian. SI – Slavonia. Tu – Tuscan. Tz – Tizia. UM – Umbria-Marche.

relationship between ostracods diversity and seawater temperature has been evidenced in other time intervals. As an example, in the Late Cretaceous of southern England, Slipper (2005) found that the high diversity of ostracods is related to regressive and cooler conditions and that the low diversity of these organisms is linked to deeper and warmer waters. Also Cronin (1991) used ostracods to estimate summer and winter ocean temperatures in the Late Pleistocene and Middle Pliocene of northwestern Atlantic.

Salinity is the main control, and very different assemblages are obtained in marine, brackish and freshwater environments (De Deckker and Forester, 1988). The ostracods found in the uppermost Pliensbachian–Lower Toarcian deposits of the Iberian Range are fully marine species and did not show any morphological features that allow considering changes in salinity (Arias, 2007, 2008). Water temperature is known to be one of the main factors controlling the ostracods distribution, and changes of water temperature in the past can also be reflected in the fossil ostracods assemblages (Arias, 2007). The cross plot of the Early Toarcian cumulative First Appearances Datum (FADs) and Last Appearances Datum (LADs) of the different ostracods taxa against the ammonites zones and subzones and the seawater palaeotemperature curve (Fig. 12b), shows that at the onset of the Toarcian, the difference between the cumulative number of FADs and LADs is not very pronounced. However, as seawater temperature rose, the number of LADs substantially increased and the cumulative number of disappearances became progressively much higher than the cumulative number of new appearances. The difference between both values reaches its maximum value around the Tenuicostatum–Serpentinum zonal transition, representing a severe decline in diversity that marks the extinction interval.

Above the extinction boundary, the cumulative number of LADs tend to stabilize, showing a vertical trend (Fig. 12b), while the number of new appearances continues to grow, representing the population interval and hence the recovery of the ostracods assemblages that inhabited the Iberian platform system. At the onset of this recovery interval, the cumulative number of FADs is still lower than the number of LADs, but the difference tends to decrease during the Serpentinum Biochron, except for the top of this interval, where a new marked increase in the number of disappearances occurred. At the Middle Toarcian Bifrons Zone, a new gradual diversification took place, although it did not compensate for the previous decline. The marked parallelism between the calculated seawater temperature and the ostracods LADs and FADs curves strongly supports the link between the recorded Early Toarcian warming and the mass extinction, illustrated here by the distribution of ostracods (Fig. 12b).

5.5. *Paleogeography, migration routes and ostracods mass extinction*

Through the Early–Middle Pliensbachian, a continuous arrival of Tethyan ostracod faunas into the European epicontinental sea (EES) occurred, marking a maximum of the Tethyan influence. The cooling interval recorded in the Late Pliensbachian and in the earliest Toarcian represented the end of invasion of Tethyan ostracod faunas into the EES, but a continuous southward expansion from the northern parts of the EES into the Iberian platform system was clearly recorded (Arias, 2007). As a preliminary hypothesis, the earliest Toarcian cooling intervals could have possibly been enhanced by the action of southwards currents following the predominant wind and currents direction trough the transcontinental Laurasian Seaway, as modelled by Bjerrum et al. (2001) and Arias (2007) (Fig. 13a). This would favour the arrival of cold waters from the Artic to the lower latitudes where the Iberian platform system was located, favouring the expansion of the ostracod faunas from the northern part of the EES and the cooling of the water masses (Arias, 2007).

However, during the subsequent Early Toarcian warming interval, these southward currents impeded the northward migration of the ostracods towards cooler waters and, as a consequence, this faunistic group, as well as many other groups, suffered a progressive disappearance that resulted in massive extinction. This faunal turnover specially affected communities of benthic organisms, but also the nektonic organisms, such as the ammonites (Cecca and Macchioni, 2004), were severely affected by this climate change. The calculated increase in temperature during the earliest Toarcian Tenuicostatum Biochron, of a duration of 300 kyr (Ogg, 2004) was responsible for a dramatic decrease in the number of taxa of ostracods at the Iberian platform system that varies between the 77% detected in the Sierra Palomera section and the 85% calculated for the La Almunia section. This remarkable loss supports a plausible cause/effect relationship between rapid warming and the ostracod mass extinction.

As faunal extinctions in the marine realm occurred at a broad time scale near the time of deposition of black shale organic-rich facies marking the ETOAE, many authors have indicated that this event may represent the acme of a long-term environmental crisis that affected the benthic fauna (Little and Benton, 1995; Harries and Little, 1999; Pálfy and Smith, 2000; Wignall, 2001; Cecca and Macchioni, 2004; Wignall et al., 2005, 2006; Arias, 2007, 2008). Nevertheless, no synchronism between the extinction event and the possible indicators of anoxia in the studied part of the Iberian platform system were found. The laminated black shale facies, indicating anoxic conditions, were well developed in central Europe, probably as a result of euxinia due to water mass stratification having a lower-salinity surface layer (McArthur et al., 2008). However, in the Iberian platform system and in many other parts of southern Europe and northern Africa, carbonate deposits are bioturbated, indicating well oxygenated environments (Savrda and Bottjer, 1986; Kemp, 1996) and did not developed organic-rich deposits except for local and ephemeral sub-basins, where TOC values are commonly lower than 1 wt.% (Fig. 13b). The two samples containing more than 1 wt.% TOC found at the Sierra Palomera section correspond to the lowermost Toarcian Mirabile Subzone and to the transition between the Mirabile and Semicelatum subzones. That means that the deposition of organic matter took place about 100 kyr before the extinction boundary. As a consequence, no direct cause/effect can be established between the possible anoxic conditions and the mass extinction. In addition, the ETOAE cannot explain why the incursion of the Tethyan ostracod faunas into the EES ceased or why the direction of ostracod migration changed (Arias, 2007).

Similar results are obtained when comparing the clearly diachronous age of the onset and termination of organic-rich black shale deposition at the ammonite zone and subzone scale in the UK (Wignall et al., 2005) and the relatively organic facies (<5 wt.%TOC) in the different European sub-basins (Gómez et al., 2008), which only occasionally coincides with the extinction boundary. Deposition of bituminous facies ended before the Tenuicostatum–Serpentinum extinction boundary in the Umbria-Marche Basin of Central Italy (Bartolini et al., 1992; Monaco et al., 1994; Parisi et al., 1996; Bucefalo Palliani et al., 1998; Mattioli et al., 2004; Mailliot et al., 2006), in the Ionian Basin of Greece, (Pettinelli et al., 1997) and in the Basque–Cantabrian Basin of Northern Spain (Comas-Rengifo et al., 1988; Rosales et al., 2004; Tremolada et al., 2005). On the contrary, deposition of the black shale facies started slightly before the extinction boundary in many other areas as in Yorkshire of the UK (Howarth, 1962; Little and Benton, 1995; Hesselbo and Jenkyns, 1995; Sælen et al., 1996; Harries and Little, 1999; Jenkyns, 2003; Wignall et al., 2005; Kemp et al., 2005; Hesselbo et al., 2007a), in southwestern Germany (Schouten et al., 2000; Röhl et al., 2001; Schmid-Röhl et al., 2002) and developed after the extinction interval. In Asturias in northern Spain, a thin laminated interval containing <5 wt.% TOC develops around the Tenuicostatum–Serpentinum extinction boundary, but the extinction interval is recorded in bioturbated facies (Gómez et al., 2008). It seems clear that a cause/effect relationship cannot be established between the onset of anoxia (deposition of laminated black shale facies) and mass extinction. In addition, the mass extinction has been recorded in many areas where no laminated black shale facies were deposited, like the examples presented here (Fig. 12b), where bioturbated deposits do not show evidences of anoxic conditions, and in the areas were laminated black shale facies are present, they postdate the extinction interval. Within the difficulties inherent to interpret the origin of the Early Toarcian mass extinction, presented data points to warming, and the subsequent effects derived from the increase in temperature, as the main cause of extinction, while global anoxia can be discarding as the overall reason for the Early Toarcian biotic crisis.

6. Conclusions

Data presented in this work provide a record of the latest Pliensbachian and the Early Toarcian seawater palaeotemperatures of the Iberian platform system. Palaeotemperatures measured in diagenetically screened belemnites from the uppermost Pliensbachian Spinatum Zone of about 13 °C in the La Almunia section, 12 °C in the Basque–Cantabrian Basin (Rosales et al., 2004) and 11.6 °C at Asturias (Gómez et al., 2008) can be considered low for a palaeolatitude of central Spain of about 35° during the Toarcian (Osete et al., 2000, in press). Close coincidence of low oceanic palaeotemperatures recorded in the UK and in Germany (Bailey et al., 2003) as well as in Spain (Rosales et al., 2004; Gómez et al., 2008; this work) confirm that the latest Pliensbachian and the earliest Toarcian represent a relative cool interval.

The seawater temperatures for the Iberian platform system started a progressive but marked increase during the Tenuicostatum Biochron, when average temperatures of 16.3 °C in the La Almunia section were reached. That represents a ΔT of 3 °C in about 300 kyr. During the Early Toarcian Tenuicostatum Biochron, coinciding with the onset of the warming interval, a dramatic decrease in the number of taxa of ostracods, of 77% (Sierra Palomera section) and 85% (La Almunia section), marked the extinction interval. The warming process accelerated around the Tenuicostatum–Serpentinum zonal boundary, coinciding with the extinction boundary. During the Serpentinum and most of the Bifrons biochrons, average temperatures of 24 °C in the La Almunia section were recorded. These temperatures can be considered as higher than the temperatures recorded in similar latitudes of the current oceans (20–21 °C according to NOAA) for the palaeolatitude of Iberia during the Toarcian. Evaluation of the values obtained in the studied sections, indicates that no other intervening factors, like a salinity increase, which would produce lower $\delta^{18}O$ values and hence higher apparent temperatures, are needed to explain the recorded temperatures. Indeed, no significant changes in salinity are reflected by the ostracods during the considered time interval in the surveyed area.

The total recorded ΔT from the Tenuicostatum to the Bifrons biochrons is in the order of 8 °C in the La Almunia section, which supports a plausible cause/effect relationship between climate change and mass extinction. The rapid warming that occurred through the Tenuicostatum Zone and amplified around the Tenuicostatum–Serpentinum zonal boundary, which was synchronously recorded at least in the different areas of Western Europe, represented a dramatic change in the environmental conditions that seriously damaged the populations of diverse organisms. The crisis affected many benthic but also nektonic organisms and pelagic producers (Mattioli et al., 2009), as the significant increase in temperature probably surpassed the temperature tolerance of numerous species that thrived in the cooler waters of the latest Pliensbachian. The progressive warming provoked the gradual disappearance of numerous taxa of ostracods and many other faunistic groups. The prevalence of southwards winds and currents in the Laurasian seaway (Chandler et al., 1992; Bjerrum et al., 2001; Arias, 2007) may have impeded the migration of the ostracods towards cooler waters located north of the Iberian platform system, as indicated by the predominant southwards migration routes detected in this area for the Early Toarcian ostracods (Arias, 2006, 2007).

Acknowledgements

We gratefully acknowledge Editor Andreas Mackensen and Reviewers Dr. Joachim Schönfel and Dr. David J. Horne and an anonymous reviewer, for their valuable comments and suggestions, which largely contributed to the improvement of the manuscript. This research work was financed by projects CGL2008-03112 and CGL2008-01273 of the Spanish Ministerio de Educación y Ciencia, and by projects CCG07-UCM/AMB-2478 and CCG07-UCM/AMB-2132.

Appendix A. Suplementary data

Supplementary data associated with this article can be found, in the online version at doi:10.1016/j.marmicro.2010.02.001.

References

Aberham, M., Baumiller, T.K., 2003. Selective extinction among Early Jurassic bivalves: a consequence of anoxia. Geology 31, 1077–1080.

Aberhan, M., Fürsich, F.T., 1997. Diversity analysis of Lower Jurassic bivalves of the Andean Basin and the Pliensbachian—Toarcian mass extinction. Lethaia 29, 181–195.

Anderson, T.F., Arthur, M.A., 1983. Stable isotopes of oxygen and carbon and their application to sedimentologic and paleoenvironmental problems. In: Arthur, M.A. (Ed.), Stable isotopes in sedimentary geology: SEPM Short Course, 10, pp. 1–151.

Apostolescu, V., 1959. Ostracodes du Lias du bassin de Paris. Revue Inst. Jr. Petrole 15, 795–817.

Arias, C.F., 1995. Los ostrácodos del Toarciense inferior en la Cordillera Ibérica. Ph. D. Thesis. Fac. C. Geológicas. Univ. Complutense Madrid, Spain.

Arias, C.F., 1996. Ostracods. In: Ureta, S. (Ed.), The Toarcian in the sector located between La Almunia de Doña Godina and Ricla. 1st Toarcian and 4th Aalenian working groups meeting: Fieldtrip Iberian Range, pp. 18–20.

Arias, C., 2006. Northern and Southern Hemisphere ostracod palaeobiogeography during the Early Jurassic: possible migration routes. Palaeogeogr. Palaeoclimatol. Palaeoecol. 233, 63–95.

Arias, C., 2007. Pliensbachian—Toarcian ostracod biogeography in NW Europe: evidence for water mass structure evolution. Palaeogeogr. Palaeoclimatol. Palaeoecol. 251, 398–421.

Arias, C.F., Comas-Rengifo, M.J., Goy, A., Herrero, C., Ruget, C., 1992. Variations dans les associations de brachiopodes, foraminifêres et ostracodes du Toarcien basal dans un secteur central de la Cordillère Ibérique. Un example dans la "Rambla del Salto" (Teruel, Espagne): Cahiers Univ. Catho. Lyon, sér. Sci., 5, pp. 5—25–5—25.

Ayress, M.A., De Deckker, P., Coles, G.P., 2004. A taxonomic and distributional survey of marine benthonic Ostracoda off Kerguelen and Heard Islands, South Indian Ocean. J. Micropalaeontol. 23, 15–38.

Bailey, T.R., Rosenthal, Y., McArthur, J.M., van de Schootbrugge, B., Thirlwall, M.F., 2003. Paleoceanographic changes of the Late Pliensbachian—Early Toarcian interval: a possible link to the genesis of an Oceanic Anoxic event. Earth Planet. Sci. Lett. 212, 307–320.

Bartolini, A., Nocchi, M., Baldanza, A., Parisi, G., 1992. Benthic life during the Early Toarcian anoxic event in the Southwestern Tethyan Umbria-Marche Basin, Central Italy. Studies in Benthic Foraminifera, Benthos'90. Tokai University Press, Sendai, Japan, pp. 323–338.

Bassoullet, J.P., Baudin, F., 1994. Le Toarcien inférieur: une période de crise dans les bassins et sur les plate-formes carbonatées de l'Europe du Nord-Ouest et de la Téthys. Geobios Mém. Spec. 17, 645–654.

Bassoullet, J.P., Lachkar, G., Baudin, F., Benshili, K., Blanc, P., Boutakiout, M., Depéche, F., Elmi, S., Ruget, C., 1991. Stratigraphie intégrée dans le Toarcien du Maroc (rides sud-rifaines et Moyen Atlas). Bull. Soc. géol. France 162, 825–839.

Bates, R.L., Jackson, J.A., 1987. Glossary of geology. American Geological Institute, Alexandria, Virginia, USA.

Benson, R., Del Grosso, R., Steineck, P., 1983. Ostracode distribution and biofacies, Newfoundland continental slope and rise. Micropaleontology 29, 430 –453.

Benton, M.J., Twitchett, R.J., 2003. How to kill (almost) all life: the end-Permian extinction event. Trends Ecol. Evol. 18, 358–365.

Bernad, J., 1996. Bivalves. In: Ureta, S. (Ed.), The Toarcian in the sector located between La Almunia de Doña Godina and Ricla. 1st Toarcian and 4th Aalenian working groups meeting: Fieldtrip Iberian Range, pp. 14–15.

Bjerrum, C.J., Surlyk, F., Callomon, J.H., Slingerland, R.L., 2001. Numerical paleoceanographic study of the Early Jurassic Transcontinental Laurasian Seaway. Paleoceanography 16, 390–404.

Boomer, I., Lord, A., Crasquin, S., 2008. The extinction of the Metacopina (Ostracoda). Senck. Lethaea 88 (1), 47–53.

Bucefalo Palliani, R., Cirilli, S., Mattioli, E., 1998. Phytoplankton response and geochemical evidence of the lower Toarcian relative sea level rise in the Umbria-Marche basin (Central Italy). Palaeogeogr. Palaeoclimatol. Palaeoecol. 142, 33–50.

Cecca, F., Macchioni, F., 2004. The two Early Toarcian (Early Jurassic) extinction events in ammonoids. Lethaia 37, 35–56.

Chandler, M.A., Rind, D., Ruedy, R., 1992. Pangaean climate during the Early Jurassic: GCM simulations and the sedimentary record of paleoclimate. Geol. Soc. Am. Bull. 104, 543–559.

Comas-Rengifo, M.J., Goy, A., Rivas, P., Yébenes, A., 1988. El Toarciense en Castillo Pedroso (Santander). Ciencias de la Tierra. Geología 11, 63–71.

Comas-Rengifo, M.J., Gómez, J.J., Goy, A., Arias, C.F., Bernad, J., García Joral, F., Herrero, C., Martínez, G., Perilli, N., 1996. The Toarcian in the Rambla del Salto (Sierra Palomera) section. In: Ureta, S. (Ed.), 1st Toarcian and 4th Aalenian working groups meeting: Fieldtrip Iberian Range, pp. 27–48.

Courtillot, V., Gaudemer, Y., 1996. Effects on mass extinction on biodiversity. Nature 381, 146–148.

Cronin, T.M., 1991. Pliocene shallow water paleoceanography of the North Atlantic Ocean based on marine ostracods. Quat. Sci. Rev. 10, 175–188.

Cronin, T.M., Holtz Jr., T.R., Whatley, R.C., 1994. Quaternary paleoceanography of the deep Arctic Ocean based on quantitative analysis of Ostracoda. Mar. Geol. 119, 305–332.

Cronin, T., Holtz Jr., T.R., Stein, Spielhagen, R., Futterer, D., Wollenburg, J., 1995. Late Quaternary paleoceanography of the Eurasian Basin, Arctic Ocean. Paleoceanography 10, 259–281.

Cronin, T., Boomer, I., Dwyer, G.S., Rodriguez-Lazaro, J., 2002. Ostracoda and paleoceanography. In: Holmes, J.A., Chivas, A.R. (Eds.), The Ostracoda: Applications in Quaternary Research. American Geophysical Union, Washington, DC, pp. 99–119.

Culver, S.J., Rawson, P.F. (Eds.), 2000. Biotic response to global change: the last 145 million years. Cambridge University Press, UK.

De Deckker, P., Forester, R.M., 1988. The use of ostracods to reconstruct continental palaeoenvironmental records. In: De Dekker, P., Colin, J.P., Peypouquet, J.P. (Eds.), Ostracoda in the Earth Science. Elsevier, Amsterdam, pp. 175–199.

Dera, G., Pucéat, E., Pellenard, P., Neige, P., Delsate, D., Joachimski, M.M., Reisberg, L., Martinez, M., 2009. Water mass exchange and variations in seawater temperature in the NW Tethys during the Early Jurassic: evidence from neodymium and oxygen isotopes of fish teeth and belemnites. Earth Planet. Sci. Lett. 286, 198–207.

Dingle, R.V., Lord, A., 1990. Benthic ostracods and deep water-masses in the Atlantic Ocean. Palaeogeogr. Palaeoclimatol. Palaeoecol. 80, 213–235.

Drexler, E., 1958. Foraminiferen und Ostracoden aus dem Lias von Siebeldingen Pfalz. Geol. Jb 75, 475–554.

Duarte, L.V., 1998. Clay minerals and geochemical evolution in the Toarcian—Lower Aalenian of the Lusitanian Basin (Portugal). Cuad. Geol. Ibérica 24, 69–98.

Fraiser, M.L., 2009. Understanding ancient, modern and future biotic responses to environmental change. Global Planet. Change 65, 105–106.

García Joral, F., Goy, A., 1996. Brachiopods. In: Ureta, S. (Ed.), The Toarcian in the sector located between La Almunia de Doña Godina and Ricla. 1st Toarcian and 4th Aalenian working groups meeting: Fieldtrip Iberian Range, pp. 12–14.

Golonka, J., 2006. Late Triassic and Early Jurassic palaeogeography of the World. Palaeogeogr. Palaeoclimatol. Palaeoecol. 244, 297–307.

Gómez, J.J., Fernández-López, S.R., 2004. Jurásico Medio. In: Vera, J.A. (Ed.), Geología de España. SGE-IGME, Madrid, pp. 500–503.

Gómez, J.J., Fernández-López, S.R., 2006. The Iberian Middle Jurassic carbonate-platform system: synthesis of the palaeogeographic elements of its eastern margin (Spain). Palaeogeogr. Palaeoclimatol. Palaeoecol. 236, 190–205.

Gómez, J.J., Goy, A., 2004. Jurásico Inferior. In: Vera, J.A. (Ed.), Geología de España. SGE-IGME, Madrid, pp. 495–500.

Gómez, J.J., Goy, A., 2005. Late Triassic and Early Jurassic palaeogeographic evolution and depositional cycles of the Wetern Tethys Iberian platform system (Eatern Spain). Palaeogeogr. Palaeoclimatol. Palaeoecol. 222, 77–94.

Gómez, J.J., Goy, A., Canales, M.L., 2008. Seawater temperature and carbon isotope variations in belemnites linked to mass extinction during the Toarcian (Early Jurassic) in Central and Northern Spain. Comparison with other European sections. Palaeogeogr. Palaeoclimatol. Palaeoecol. 258, 28–58.

Gómez, J.J., Canales, M.L., Ureta, S., Goy, A., 2009. Palaeoclimatic and biotic changes during the Aalenian (Middle Jurassic) at the southern Laurasian Seaway (Basque–Cantabrian Basin, northern Spain). Palaeogeogr. Palaeoclimatol. Palaeoecol. 275, 14–27.

Goy, A., Martínez, G., 1990. Biozonación del Toarciense en el área de la Almunia de Doña Godina-Ricla (Sector Central de la Cordillera Ibérica). Cuad. Geol. Ibér. 14, 11–53.

Goy, A., Martínez, G., Arias, C.F., Bernad, J., García Joral, F., Gómez, J.J., Herrero, C., Perilli, N., Ureta, S., 1996. The Toarcian in the sector located between La Almunia de Doña Godina and Ricla. In: Ureta, S. (Ed.), 1st Toarcian and 4th Aalenian working groups meeting: Fieldtrip Iberian Range, pp. 3–23.

Cavazza, W., Roure, F.M., Spakman, W., Stampfli, G.M., Ziegler, P.A., (Eds.), The TRANSMED Atlas–The Mediterraean Region from Crust to Mantle. Springer Berlin Heidelberg New York, pp. 53–80 and CD-ROM.

Suan, G., Mattioli, E., Pittet, B., Maillot, S., Lécuyer, C., 2008. Evidence for major environmental perturbation prior to and during the Toarcian (Early Jurassic) Oceanic Anoxic Event from the Lusitanian Basin, Portugal. Paleoceanography 23, PA 1202. doi:10.1029/2007PA001459.

Tremolada, F., van de Schootbrugge, B., Erba, E., 2005. Early Jurassic schizosphaerellid crisis in Cantabria, Spain: Implications for calcification rates and phytoplankton evolution across the Toarcian oceanic anoxic event. Paleoceanography 20, PA211. doi:10.1029/2004PA001120.

van de Schootbrugge, B., McArthur, J.M., Bailey, T.R., Rosenthal, Y., Wright, J.D., Miller, K.G., 2005. Toarcian oceanic anoxic event: an assessment of global causes using belemnite C isotope records. Paleoceanography 20, PA3008. doi:10.1029/2004PA001102.

Vera, J.A., 2001. Evolution of the South Iberian Continental margin. In: Ziegler, P.A., Cavazza, W., Robertson, A.H.F., Crasquin-Soleau, S. (Eds.), Pery-Tethys Memoir 6: Peri-Thetyan Rift/Wrench Basins and Passive Margins: Mém. Mus. natn. Hist. nat., 186, pp. 109–143.

Voigt, S., Gale, A.S., Voigt, T., 2006. Sea-level change, carbon cycling and palaeoclimate during the Late Cenomanian of northwest Europe; an integrated palaeoenvironmental analysis. Cretac. Res. 27, 836–858.

Vörös, A., 2002. Victims of the Early Toarcian anoxic event: the radiation and extinction of Jurassic Koninckinidae (Brachiopoda). Lethaia 35, 345–357.

Whatley, R.C., 1988. Ostracoda and palaeogeography. In: Deckker, P., Colin, J.P., Peypouquet, J.P. (Eds.), Ostracoda in the Earth Science. Elsevier, Amsterdam.

Wignall, P.B., 2001. Large igneous provinces and mass extinctions. Earth-Sci. Rev. 53, 1–33.

Wignall, P.B., Newton, R.J., Little, C.T.S., 2005. The timing of paleoenvironmental change and cause-and-effect relationships during the early Jurassic mass extinction in Europe. Am. J. Sci. 305, 1014–1032.

Wignall, P.B., McArthur, J.M., Little, C.T., Hallam, A., 2006. Methane release in the Early Jurassic period. Nature 441, E5 Comments to Kemp et al., 2005.

Wright, E.K., 1987. Stratification and paleocirculation of the Late Cretaceous Western Interior Seaway of North America. Geol. Soc. Am. Bull. 99, 480–490.

Ziegler, P.A., 1990. Geological Atlas of Western and Central Europe, 2nd edition. Shell Internationale Petroleum Maatschappij, The Hague.